

Tyler Thorsen

David Winker, Richard Ferrare, Seiji Kato

NASA Langley Research Center

Uncertainty in observational estimates of the aerosol direct radiative effect and forcing

Introduction

- Aerosols continue to be responsible for the largest uncertainty in determining the anthropogenic radiative forcing of the climate
- Aerosols influence anthropogenic forcing indirectly via modifications to cloud properties as well as directly through the scattering and absorption of solar radiation— the aerosol direct radiative forcing (DRF, aka $\mathrm{RF}_{\mathrm{ari}}$)

Introduction

- Aerosols continue to be responsible for the largest uncertainty in determining the anthropogenic radiative forcing of the climate
- Aerosols influence anthropogenic forcing indirectly via modifications to cloud properties as well as directly through the scattering and absorption of solar radiation— the aerosol direct radiative forcing (DRF, aka $\mathrm{RF_{ari}}$)
- IPCC AR5: aerosol DRF ($\mathrm{RF_{ari}}$) $= -0.35 \pm 0.5$ Wm^{-2} (95% confidence). Evidence that the IPCC assessment underestimates the true uncertainty. (Samset et al., 2014; Loeb and Su, 2010)

Introduction

- Aerosols continue to be responsible for the largest uncertainty in determining the anthropogenic radiative forcing of the climate
- Aerosols influence anthropogenic forcing indirectly via modifications to cloud properties as well as directly through the scattering and absorption of solar radiation— the aerosol direct radiative forcing (DRF, aka $\mathrm{RF_{ari}}$)
- IPCC AR5: aerosol DRF ($\mathrm{RF_{ari}}$) $= -0.35 \pm 0.5$ Wm^{-2} (95% confidence). Evidence that the IPCC assessment underestimates the true uncertainty. (Samset et al., 2014; Loeb and Su, 2010)
- From observations, the aerosol direct radiative effect (DRE)— the radiative effect of all aerosols both natural and anthropogenic— is more readily quantifiable (Boucher and Tanré, 2000; Bellouin et al., 2003, 2005; Loeb and Manalo-Smith, 2005; Zhang, 2005; Remer and Kaufman, 2006; Yu et al., 2006; Zhao et al., 2008, 2011; Henderson et al., 2013; Oikawa et al., 2013; Oh et al., 2013; Lee et al., 2014; Matus et al., 2015; Lacagnina et al., 2017; Oikawa et al., 2018; Korras-Carraca et al., 2019; Matus et al., 2019)
  - These DRE estimates produce a wide range of values
  - Estimates often don't agree within their stated uncertainties

Introduction

- Aerosols continue to be responsible for the largest uncertainty in determining the anthropogenic radiative forcing of the climate
- Aerosols influence anthropogenic forcing indirectly via modifications to cloud properties as well as directly through the scattering and absorption of solar radiation— the aerosol direct radiative forcing (DRF, aka $\mathrm{RF_{ari}}$)
- IPCC AR5: aerosol DRF ($\mathrm{RF_{ari}}$) $= -0.35 \pm 0.5$ Wm^{-2} (95% confidence). Evidence that the IPCC assessment underestimates the true uncertainty. (Samset et al., 2014; Loeb and Su, 2010)
- From observations, the aerosol direct radiative effect (DRE)— the radiative effect of all aerosols both natural and anthropogenic— is more readily quantifiable (Boucher and Tanré, 2000; Bellouin et al., 2003, 2005; Loeb and Manalo-Smith, 2005; Zhang, 2005; Remer and Kaufman, 2006; Yu et al., 2006; Zhao et al., 2008, 2011; Henderson et al., 2013; Oikawa et al., 2013; Oh et al., 2013; Lee et al., 2014; Matus et al., 2015; Lacagnina et al., 2017; Oikawa et al., 2018; Korras-Carraca et al., 2019; Matus et al., 2019)
  - These DRE estimates produce a wide range of values
  - Estimates often don't agree within their stated uncertainties

Comprehensive probe into the sensitivities in calculating the aerosol DRE/DRF and an assessment of uncertainties in observation-based estimates.

Introduction: approach

1. Compute aerosol DRE/DRF partial derivatives / Jacobians / radiative kernels ($\partial DRX/\partial x$)
   - Built a generic framework for assessing uncertainties
2. Apply kernels mainly to the systematic uncertainties found in AERONET: (Δx)
   - Global constraints only possible with satellite remote sensing + AERONET uncertainty $<<$ satellite uncertainty $=$ **Lower-bound on the current observational uncertainty in the aerosol DRE/DRF**
     - Optimistic uncertainty assessment compared to a literature survey of past (satellite-based) estimates

---

1. Thorsen, T. J., R. A. Ferrare, S. Kato, and D. M. Winker, 2020: Aerosol Direct Radiative Effect Sensitivity Analysis. J. Climate, 33, 6119-6139 doi:10.1175/jcli-d-19-0669.1
2. Thorsen, T. J., D. M. Winker, and R. A. Ferrare: Uncertainty in observational estimates of the aerosol direct radiative effect and forcing. J. Climate, in press doi:10.1175/jcli-d-19-1009.1

Introduction: approach

1. Compute aerosol DRE/DRF partial derivatives / Jacobians / radiative kernels ($\partial DRX/\partial x$)
   - Built a generic framework for assessing uncertainties
2. Apply kernels mainly to the systematic uncertainties found in AERONET: (Δx)
   - Global constraints only possible with satellite remote sensing + AERONET uncertainty << satellite uncertainty = **Lower-bound on the current observational uncertainty in the aerosol DRE/DRF**
     - Optimistic uncertainty assessment compared to a literature survey of past (satellite-based) estimates
   - $\sigma_{DRX}(t,i,j) = ... + \frac{\partial DRX}{\partial x}\Delta x + ...$
   - σ_{DRX}: total aerosol DRE/DRF uncertainty resolved for a single year, every three hours (t), on a 2.5 degree grid (i,j) [mostly focus on the global mean uncertainty]
   - Δx: one standard deviation (1σ) systematic (non-random) uncertainties

---

1. Thorsen, T. J., R. A. Ferrare, S. Kato, and D. M. Winker, 2020: Aerosol Direct Radiative Effect Sensitivity Analysis. J. Climate, 33, 6119-6139 doi:10.1175/jcli-d-19-0669.1
2. Thorsen, T. J., D. M. Winker, and R. A. Ferrare: Uncertainty in observational estimates of the aerosol direct radiative effect and forcing. J. Climate, in press doi:10.1175/jcli-d-19-1009.1

Observational uncertainties: aerosol optical properties

$$\sigma_{DRX}(t,i,j) = \left[\left(\frac{\partial DRX}{\partial AOD} \boldsymbol{\Delta AOD} - \frac{\partial DRX}{\partial SSA} \boldsymbol{\Delta SSA} \right)^2 + \left(\frac{\partial DRX}{\partial g} \boldsymbol{\Delta g} \right)^2 + \ldots \right.$$

- AOD, SSA, asymmetry factor uncertainties are based those found in the AERONET database
- **Hypothetical global observing system with AERONET-like accuracy:**
  - Uncertainties from the fixed AERONET sites are extrapolated globally
  - Same uncertainties for both all-sky and clear-sky conditions.

Observational uncertainties: aerosol optical properties

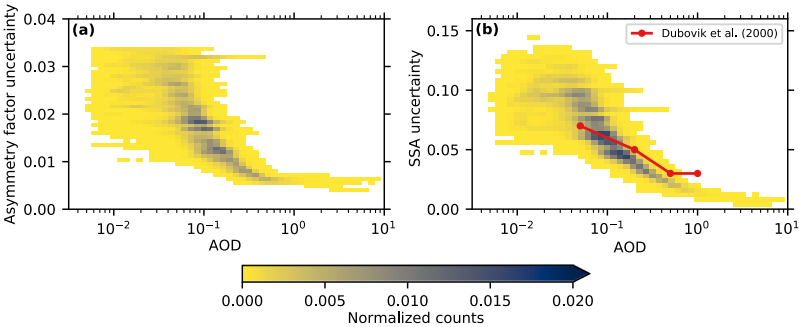
$$\sigma_{DRX}(t,i,j) = \left[\left(\frac{\partial DRX}{\partial AOD} \boldsymbol{\Delta AOD} - \frac{\partial DRX}{\partial SSA} \boldsymbol{\Delta SSA} \right)^2 + \left(\frac{\partial DRX}{\partial g} \boldsymbol{\Delta g} \right)^2 + \ldots \right.$$

- AOD, SSA, asymmetry factor uncertainties are based those found in the AERONET database
- **Hypothetical global observing system with AERONET-like accuracy:**
  - Uncertainties from the fixed AERONET sites are extrapolated globally
  - Same uncertainties for both all-sky and clear-sky conditions.
- Extrapolating the AOD uncertainty globally is trivial: $\Delta AOD = 0.01$

Observational uncertainties: aerosol optical properties

$$\sigma_{DRX}(t,i,j) = \left[\left(\frac{\partial DRX}{\partial AOD}\boldsymbol{\Delta AOD} - \frac{\partial DRX}{\partial SSA}\boldsymbol{\Delta SSA}\right)^2 + \left(\frac{\partial DRX}{\partial g}\boldsymbol{\Delta g}\right)^2 + \ldots\right.$$

- AOD, SSA, asymmetry factor uncertainties are based those found in the AERONET database
- **Hypothetical global observing system with AERONET-like accuracy:**
  - Uncertainties from the fixed AERONET sites are extrapolated globally
  - Same uncertainties for both all-sky and clear-sky conditions.
- Extrapolating the AOD uncertainty globally is trivial: $\Delta AOD = 0.01$
- ΔSSA, Δg need a more substantial effort needed to extrapolate these globally:
  - For each data points in the MERRA-2 data, select a representative SSA and asymmetry factor uncertainty from the AERONET aerosol inversion uncertainty data product ("U27" product)



Observational uncertainties: non-aerosol properties

$$\sigma_{DRX}(t,i,j) = \Bigg[\left(\frac{\partial DRX}{\partial AOD}\Delta AOD - \frac{\partial DRX}{\partial SSA}\Delta SSA\right)^2 + \left(\frac{\partial DRX}{\partial g}\Delta g\right)^2 + \ldots$$
$$\left(\frac{\partial DRX}{\partial a}\boldsymbol{\Delta a}\right)^2 + \left(\frac{\partial DRX}{\partial COD}\boldsymbol{\Delta COD}\right)^2 + \left(\frac{\partial DRF}{\partial f_{ant}}\boldsymbol{\Delta f_{ant}}\right)^2 + \ldots$$

Taken from literature:

- $\Delta a(land)$: land surface albedo uncertainty $= 0.02$
  (Jin et al., 2003; Cescatti et al., 2012; Roman et al., 2013; Stroeve et al., 2013; Wang et al., 2014)
- $\Delta a(ocean)$: ocean surface albedo uncertainty $= 8\%$ (Jin et al., 2004, 2005)
- ΔCOD: cloud optical depth uncertainty $= 25\%$ (Grosvenor et al., 2018)
- Δf_{ant}: anthropogenic fraction $= 30\%$ (Kaufman et al., 2005)

Observational uncertainties: spectral/vertical simplifications

$$\sigma_{DRX}(t,i,j) = \Bigg[\left(\frac{\partial DRX}{\partial AOD}\Delta AOD - \frac{\partial DRX}{\partial SSA}\Delta SSA\right)^2 + \left(\frac{\partial DRX}{\partial g}\Delta g\right)^2 + \ldots$$
$$\left(\frac{\partial DRX}{\partial a}\Delta a\right)^2 + \left(\frac{\partial DRX}{\partial COD}\Delta COD\right)^2 + \left(\frac{\partial DRF}{\partial f_{ant}}\Delta f_{ant}\right)^2 + \ldots$$
$$\left(\boldsymbol{\sigma^{z}_{DRX}} + \boldsymbol{\sigma^{H}_{DRX}} + \boldsymbol{\sigma^{\lambda}_{DRX}}\right)^2\Bigg]^{1/2}$$

- To compute the aerosol DRE/DRF, the aerosol optical properties need to be specified in each vertical layer (72) and across the broadband spectrum (175nm-4μm)
- AERONET sun photometers only retrieve **column-averaged** aerosol scattering properties at **limited wavelengths** (440, 675, 870, 1020 nm)

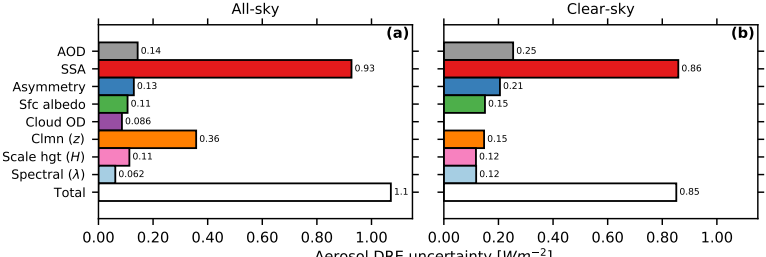
Observational uncertainties: spectral/vertical simplifications

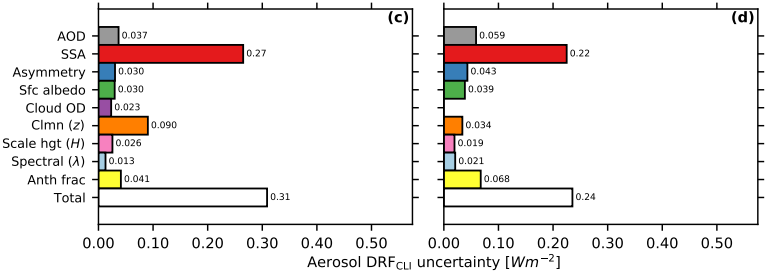
$$\sigma_{DRX}(t,i,j) = \Bigg[\left(\frac{\partial DRX}{\partial AOD}\Delta AOD - \frac{\partial DRX}{\partial SSA}\Delta SSA\right)^2 + \left(\frac{\partial DRX}{\partial g}\Delta g\right)^2 + \ldots$$
$$\left(\frac{\partial DRX}{\partial a}\Delta a\right)^2 + \left(\frac{\partial DRX}{\partial COD}\Delta COD\right)^2 + \left(\frac{\partial DRF}{\partial f_{ant}}\Delta f_{ant}\right)^2 + \ldots$$
$$\left(\boldsymbol{\sigma^{z}_{DRX}} + \boldsymbol{\sigma^{H}_{DRX}} + \boldsymbol{\sigma^{\lambda}_{DRX}}\right)^2\Bigg]^{1/2}$$

- To compute the aerosol DRE/DRF, the aerosol optical properties need to be specified in each vertical layer (72) and across the broadband spectrum (175nm-4μm)
- AERONET sun photometers only retrieve **column-averaged** aerosol scattering properties at **limited wavelengths** (440, 675, 870, 1020 nm)
- Using MERRA-2 vertical/spectral properties as "truth", combine the difference between the simplified properties and the "true" values with the kernels
- Assumed to be representative of 1σ systematic uncertainty

DRE/DRF global mean uncertainty

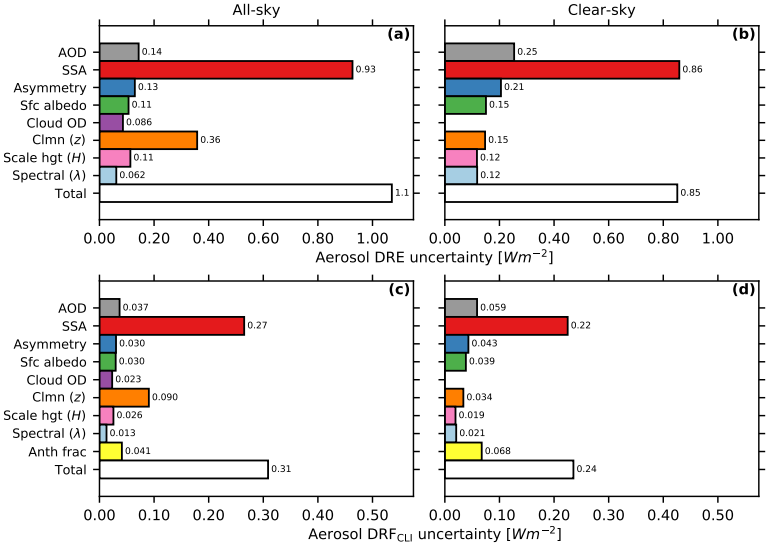
$$\left[\left(\frac{\partial DRX}{\partial AOD}\Delta AOD - \frac{\partial DRX}{\partial SSA}\Delta SSA\right)^2 + \left(\frac{\partial DRX}{\partial g}\Delta g\right)^2 + \left(\frac{\partial DRX}{\partial a}\Delta a\right)^2 + \left(\frac{\partial DRX}{\partial COD}\Delta COD\right)^2 + \left(\frac{\partial DRF}{\partial f_{ant}}\Delta f_{ant}\right)^2 + \left(\sigma^{z}_{DRX} + \sigma^{H}_{DRX} + \sigma^{\lambda}_{DRX}\right)^2\right]^{1/2}$$





DRE/DRF global mean uncertainty

$$\left[\left(\frac{\partial DRX}{\partial AOD}\Delta AOD - \frac{\partial DRX}{\partial SSA}\Delta SSA\right)^2 + \left(\frac{\partial DRX}{\partial g}\Delta g\right)^2 + \left(\frac{\partial DRX}{\partial a}\Delta a\right)^2 + \left(\frac{\partial DRX}{\partial COD}\Delta COD\right)^2 + \left(\frac{\partial DRF}{\partial f_{ant}}\Delta f_{ant}\right)^2 + \left(\sigma^{z}_{DRX} + \sigma^{H}_{DRX} + \sigma^{\lambda}_{DRX}\right)^2\right]^{1/2}$$

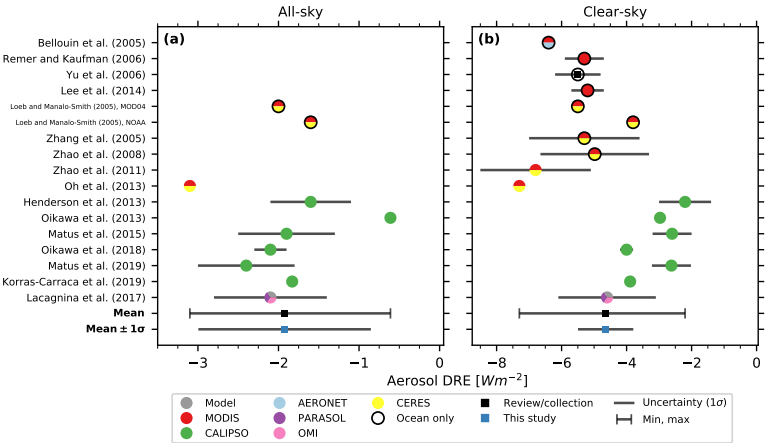


- $\sigma_{DRE} = 1.1\ Wm^{-2}$
- $\sigma_{DRF} = 0.31\ Wm^{-2}$
- Larger all-sky uncertainties: less cancellation between AOD/SSA, increased uncertainty from using column-averages
- Total uncertainty dominated by the contribution from SSA (e.g. McComiskey et al., 2008; Loeb and Su, 2010; Samset et al., 2018)

Comparison to other studies

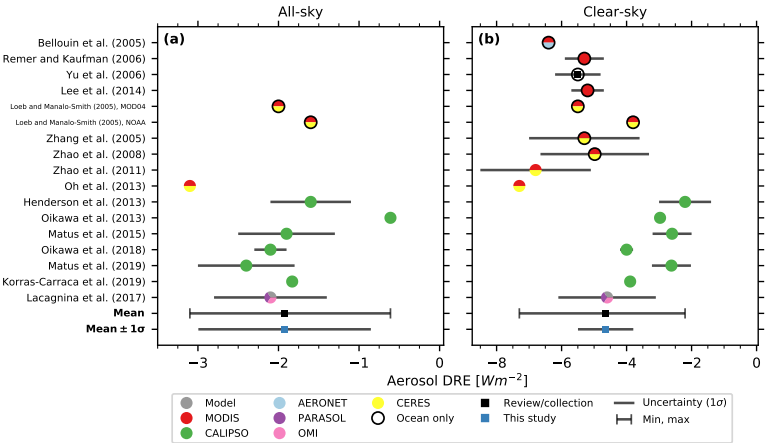
- Focus on satellite-based global estimates made in the NASA EOS era
- Uncertainty in this work is a lower bound
  (AERONET uncertainty $<<$ satellite uncertainty)
- Can only directly assess veracity of uncertainty for studies that follow the specific approach of using observed optical properties to forward model the associated broadband fluxes
  - "Broadband flux approach" (e.g. CERES) requires a completely different uncertainty assessment
  - Modeling/reanalysis can provide additional constraints as well

DRE literature comparisons



- Many of these estimates are clear-sky ocean-only (black circles) using MODIS (red); remainder use CERES or CALIPSO
- Lacagnina et al. (2017): not purely observations, but only study to use satellite-retrieved SSA
- All-sky range of surveyed values is similar to our 1σ uncertainty range, clear-sky range is much larger

DRE literature comparisons

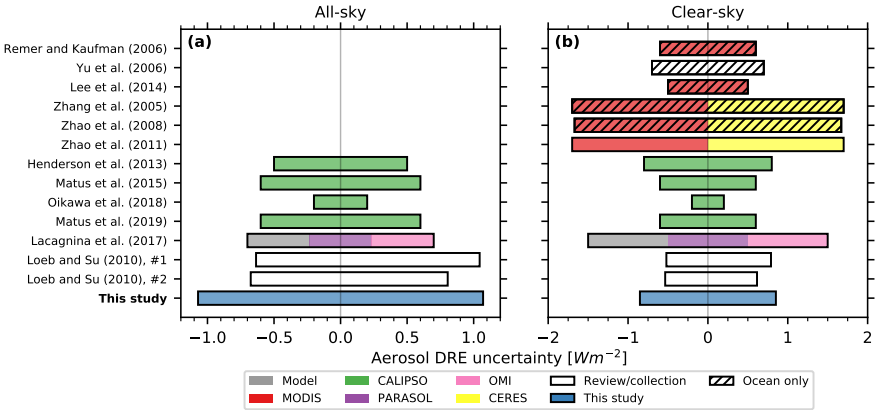


- Many of these estimates are clear-sky ocean-only (black circles) using MODIS (red); remainder use CERES or CALIPSO
- Lacagnina et al. (2017): not purely observations, but only study to use satellite-retrieved SSA
- All-sky range of surveyed values is similar to our 1σ uncertainty range, clear-sky range is much larger

Clear-sky MODIS/CALIPSO offset:

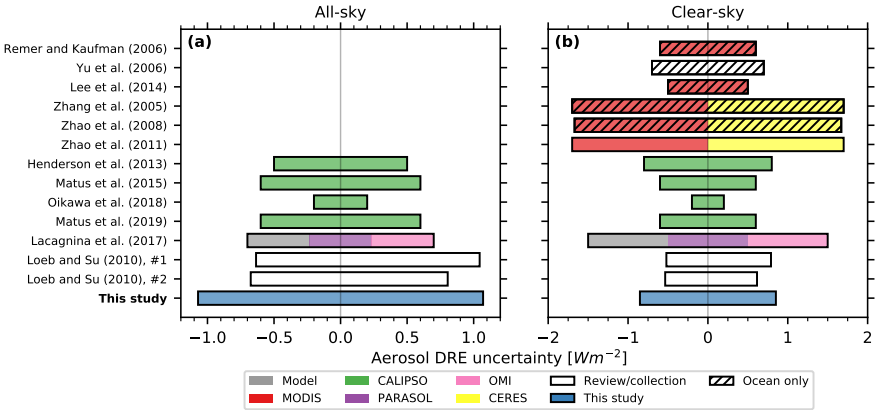
- CALIPSO sensitivity: possible 30-50% underestimation of the DRE magnitude (Thorsen et al., 2017)
- MODIS cloud contamination: possible negative DRE bias of 0.5 to 1.0 Wm^{-2} (Yu et al., 2006; Remer and Kaufman, 2006)

DRE literature comparisons: uncertainties



- All surveyed studies have smaller stated uncertainties than our estimate with the exception of the CERES-based estimates (which aren't directly comparable to our uncertainty) and the clear-sky DRE from Lacagnina et al. (2017)

DRE literature comparisons: uncertainties

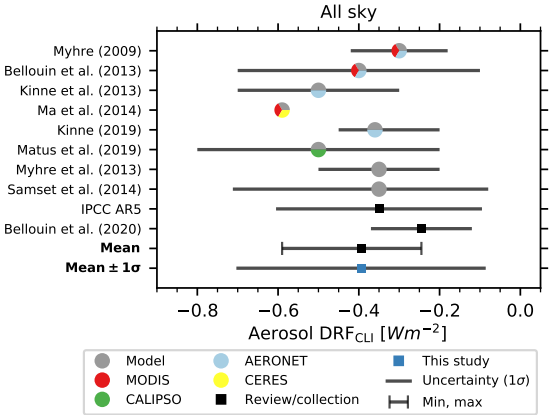


- All surveyed studies have smaller stated uncertainties than our estimate with the exception of the CERES-based estimates (which aren't directly comparable to our uncertainty) and the clear-sky DRE from Lacagnina et al. (2017)
- **Most previous studies significantly underestimate the aerosol DRE uncertainty**
  - Only Lacagnina et al. (2017) explicitly includes the contribution of the SSA uncertainty

DRF literature comparisons

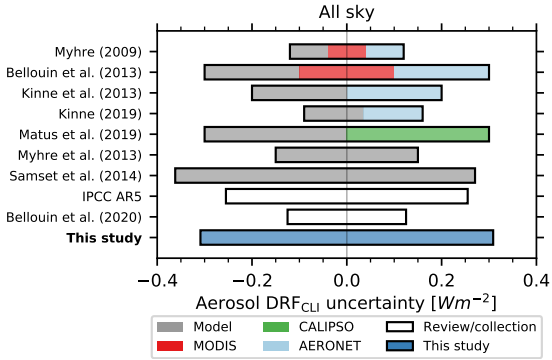
- Always going to need modeling for DRF to assess the pre-industrial reference state.
- Expanding scope of review to include studies that incorporate observations but rely on modeling to compliment the observations in various ways
- Also included are the purely model based estimates from the AeroCom Phase II experiment (Myhre et al., 2013; Samset et al., 2014) along with the expert judgment assessments from the IPCC AR5 (Boucher et al., 2013) and the Yu et al. (2006) and Bellouin et al. (2020) review papers.

DRF literature comparisons



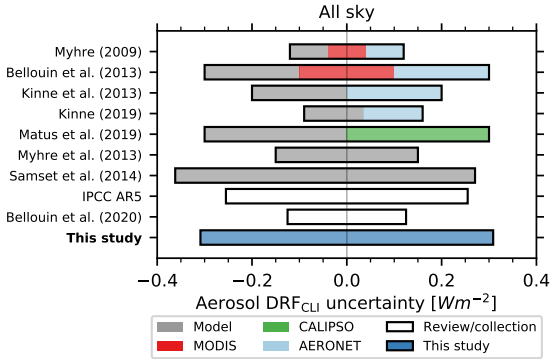
- Range of literature values fall well within our uncertainty bounds (opposite what was found with the DRE)
- Somewhat counterintuitive: expect, relative to the uncertainty in an observational constraint, that estimating DRF would produce a wider range of values than DRE
- Possible for modeling to provide additional constraints on the observations leading to a reduced range of values

DRF literature comparisons: uncertainty



- Comparable or smaller than our 1σ uncertainty range
- Cannot directly assess the validity of these literature uncertainties since modeling can provide additional constraints

DRF literature comparisons: uncertainty



- Comparable or smaller than our 1σ uncertainty range
- Cannot directly assess the validity of these literature uncertainties since modeling can provide additional constraints

---

- Past studies have underestimated the uncertainty $\rightarrow$ the aerosol DRF has been constrained to a point beyond that possible with current observational accuracies
  - Model diversity underestimates the true modeling uncertainty

  (Samset et al., 2014; Carslaw et al., 2018; Johnson et al., 2018; Yoshioka et al., 2019)
- Current observational uncertainties are too large to provide strong constraints on models

Conclusions

Lower-bound on observational uncertainty (1σ):

- Aerosol DRE uncertainty $= 1.1\ Wm^{-2}$
- Aerosol DRF uncertainty $= 0.31\ Wm^{-2}$
  - Total uncertainty dominated by the contribution from SSA

Conclusions

Lower-bound on observational uncertainty (1σ):

- Aerosol DRE uncertainty $= 1.1\ Wm^{-2}$
- Aerosol DRF uncertainty $= 0.31\ Wm^{-2}$
  - Total uncertainty dominated by the contribution from SSA

Literature comparisons:

- Most previous aerosol DRE estimates significantly uncertainty by not accounting for the impact of SSA uncertainty
- Aerosol DRF uncertainties are typically comparable to, or smaller than, our lower-bound uncertainty estimates (including the IPCC AR5 uncertainty of 0.26 Wm^{-2})
  - Past studies have underestimated the uncertainty *and/or*
    current observational uncertainties are too large to provide strong constraints

Conclusions

Lower-bound on observational uncertainty (1σ):

- Aerosol DRE uncertainty = 1.1 Wm^{-2}
- Aerosol DRF uncertainty = 0.31 Wm^{-2}
  - Total uncertainty dominated by the contribution from SSA

Literature comparisons:

- Most previous aerosol DRE estimates significantly uncertainty by not accounting for the impact of SSA uncertainty
- Aerosol DRF uncertainties are typically comparable to, or smaller than, our lower-bound uncertainty estimates (including the IPCC AR5 uncertainty of 0.26 Wm^{-2})
  - Past studies have underestimated the uncertainty *and/or* current observational uncertainties are too large to provide strong constraints

Reducing current uncertainty: (not shown)

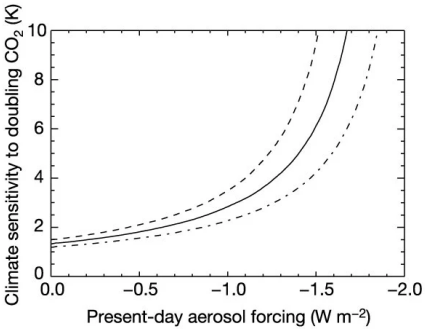
- A hypothetical (i.e. future) approach that would leverage aerosol typing and improved vertical information reduced the aerosol DRE/DRF uncertainty by about 40%

Thorsen, T. J., R. A. Ferrare, S. Kato, and D. M. Winker, 2020: Aerosol Direct Radiative Effect Sensitivity Analysis. J. Climate, 33, 6119-6139, doi:10.1175/jcli-d-19-0669.1

Thorsen, T. J., D. M. Winker, and R. A. Ferrare: Uncertainty in observational estimates of the aerosol direct radiative effect and forcing. J. Climate, in press, doi:10.1175/jcli-d-19-1009.1

Introduction

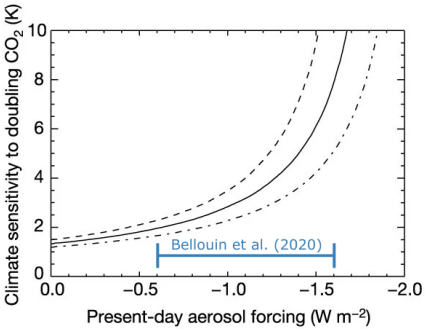
- Aerosols continue to be responsible for the largest uncertainty in determining the anthropogenic radiative forcing of the climate



(Andreae et al. 2005)

Introduction

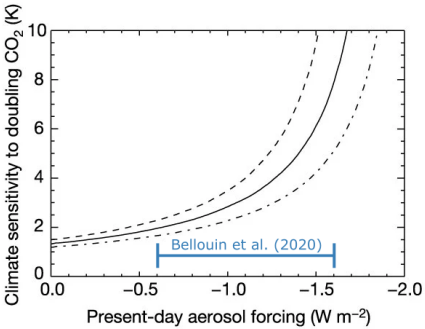
- Aerosols continue to be responsible for the largest uncertainty in determining the anthropogenic radiative forcing of the climate



(Andreae et al. 2005)

Introduction

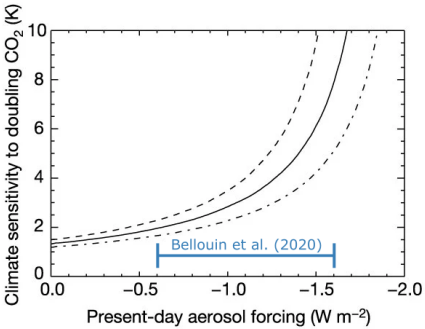
- Aerosols continue to be responsible for the largest uncertainty in determining the anthropogenic radiative forcing of the climate
- Influence anthropogenic forcing indirectly via modifications to cloud properties as well as directly through the scattering and absorption of solar radiation— the aerosol direct radiative forcing (DRF, aka $\mathrm{RF}_{\mathrm{ari}}$)



(Andreae et al. 2005)

Introduction

- Aerosols continue to be responsible for the largest uncertainty in determining the anthropogenic radiative forcing of the climate
- Influence anthropogenic forcing indirectly via modifications to cloud properties as well as directly through the scattering and absorption of solar radiation— the aerosol direct radiative forcing (DRF, aka $\mathrm{RF_{ari}}$)



(Andreae et al. 2005)

- IPCC AR5: aerosol DRF ($\mathrm{RF_{ari}}$) $= -0.35 \pm 0.5$ Wm^{-2} (95% confidence) (similar uncertainty as in AR4)
- There is evidence that the IPCC assessment underestimates the true uncertainty:
  - Samset et al. (2014): much larger uncertainty by fully sampling the variance in the relevant parameters across models (instead of using model diversity)
  - Loeb and Su (2010): **2x-4x** larger uncertainty than the IPCC AR4 assessment is implied by even the most optimistic of observational uncertainties

Introduction: satellite observations

- Aerosol DRF: can only observe proxies (e.g. fine mode fraction) for anthropogenic aerosols, those proxies are uncertain (Kaufman et al., 2005; Anderson, 2005; Bellouin et al., 2005; Christopher et al., 2006; Yu et al., 2006, 2009)

Introduction: satellite observations

- Aerosol DRF: can only observe proxies (e.g. fine mode fraction) for anthropogenic aerosols, those proxies are uncertain (Kaufman et al., 2005; Anderson, 2005; Bellouin et al., 2005; Christopher et al., 2006; Yu et al., 2006, 2009)
- The aerosol direct radiative effect (DRE)— the radiative effect of all aerosols both natural and anthropogenic— is more readily quantifiable (Boucher and Tanré, 2000; Bellouin et al., 2003, 2005; Loeb and Manalo-Smith, 2005; Zhang, 2005; Remer and Kaufman, 2006; Yu et al., 2006; Zhao et al., 2008, 2011; Henderson et al., 2013; Oikawa et al., 2013; Oh et al., 2013; Lee et al., 2014; Matus et al., 2015; Lacagnina et al., 2017; Oikawa et al., 2018; Korras-Carraca et al., 2019; Matus et al., 2019)
  - These DRE estimates produce a wide range of values: clear-sky ocean values span a 2.5 Wm^{-2} range
  - Estimates often don't agree within their stated uncertainties

Introduction: satellite observations

- Aerosol DRF: can only observe proxies (e.g. fine mode fraction) for anthropogenic aerosols, those proxies are uncertain (Kaufman et al., 2005; Anderson, 2005; Bellouin et al., 2005; Christopher et al., 2006; Yu et al., 2006, 2009)
- The aerosol direct radiative effect (DRE)— the radiative effect of all aerosols both natural and anthropogenic— is more readily quantifiable (Boucher and Tanré, 2000; Bellouin et al., 2003, 2005; Loeb and Manalo-Smith, 2005; Zhang, 2005; Remer and Kaufman, 2006; Yu et al., 2006; Zhao et al., 2008, 2011; Henderson et al., 2013; Oikawa et al., 2013; Oh et al., 2013; Lee et al., 2014; Matus et al., 2015; Lacagnina et al., 2017; Oikawa et al., 2018; Korras-Carraca et al., 2019; Matus et al., 2019)
  - These DRE estimates produce a wide range of values: clear-sky ocean values span a 2.5 Wm^{-2} range
  - Estimates often don't agree within their stated uncertainties

Comprehensive probe into the sensitivities in calculating the aerosol DRE/DRF and an assessment of uncertainties in observation-based estimates.

Introduction: approach

- Similar approach as Loeb and Su (2010) is used who calculated DRF uncertainty by perturbing 2 climatological sets of global mean aerosol and cloud properties by their respective uncertainties (AERONET-based uncertainties).

Loeb and Su (2010):



Introduction: approach

- Similar approach as Loeb and Su (2010) is used who calculated DRF uncertainty by perturbing 2 climatological sets of global mean aerosol and cloud properties by their respective uncertainties (AERONET-based uncertainties).

Loeb and Su (2010):



This study: a more detailed version of this analysis:

1. Compute aerosol DRE partial derivatives (Jacobians, radiative kernels)
   - Build a framework for assessing uncertainties
2. Apply kernels mainly to the systematic uncertainties found in AERONET
   - Global constraints only possible with satellite remote sensing + AERONET uncertainty $<<$ satellite uncertainty $=$ **Lower-bound on the current observational uncertainty in the aerosol DRE/DRF**
     - Optimistic uncertainty assessment compared to a literature survey of past (satellite-based) estimates

1. Thorsen, T. J., R. A. Ferrare, S. Kato, and D. M. Winker, 2020: Aerosol Direct Radiative Effect Sensitivity Analysis. J. Climate, 33, 6119–6139
2. Thorsen, T. J., D. M. Winker, and R. A. Ferrare: Uncertainty in observational estimates of the aerosol direct radiative effect and forcing. J. Climate, in review

Computing aerosol radiative effects

1. Aerosol direct radiative effect (DRE): difference between the present-day (PD) net **shortwave** flux F at the top of the atmosphere (TOA) with aerosols included (all-sky) and with aerosols removed (clean-sky):

$$DRE_{all} = F_{PD,all} - \boldsymbol{F_{PD,clean}} \tag{1}$$

Computing aerosol radiative effects

1. Aerosol direct radiative effect (DRE): difference between the present-day (PD) net **shortwave** flux F at the top of the atmosphere (TOA) with aerosols included (all-sky) and with aerosols removed (clean-sky):

$$DRE_{all} = F_{PD,all} - \boldsymbol{F_{PD,clean}} \tag{1}$$

2. Aerosol direct radiative forcing (DRF): difference in the net shortwave flux between calculations with present-day and pre-industrial (PI) emissions of aerosols:

$$DRF_{CLI,all} = F_{PD,all} - \boldsymbol{F_{PI,all}} \tag{2}$$

   - The "climate aerosol DRF" / $\mathrm{RF_{ari}}$: radiative effect relative to a pre-industrial reference state

Computing aerosol radiative effects

1. Aerosol direct radiative effect (DRE): difference between the present-day (PD) net **shortwave** flux F at the top of the atmosphere (TOA) with aerosols included (all-sky) and with aerosols removed (clean-sky):

$$DRE_{all} = F_{PD,all} - \boldsymbol{F_{PD,clean}} \tag{1}$$

2. Aerosol direct radiative forcing (DRF): difference in the net shortwave flux between calculations with present-day and pre-industrial (PI) emissions of aerosols:

$$DRF_{CLI,all} = F_{PD,all} - \boldsymbol{F_{PI,all}} \tag{2}$$

   - The "climate aerosol DRF" / $\mathrm{RF_{ari}}$: radiative effect relative to a pre-industrial reference state

- Equations (1)–(2) also have analogous expressions in the clear-sky

Aerosol DRE/DRF uncertainty

$$\sigma_{DRX}(t,i,j) = \Bigg[\left(\frac{\partial DRX}{\partial AOD}\Delta AOD - \frac{\partial DRX}{\partial SSA}\Delta SSA\right)^2 + \left(\frac{\partial DRX}{\partial g}\Delta g\right)^2 + \left(\frac{\partial DRX}{\partial a}\Delta a\right)^2 + \left(\frac{\partial DRX}{\partial COD}\Delta COD\right)^2 + \left(\frac{\partial DRF}{\partial f_{ant}}\Delta f_{ant}\right)^2 + \left(\sigma^z_{DRX} + \sigma^H_{DRX} + \sigma^\lambda_{DRX}\right)^2\Bigg]^{1/2}$$

Aerosol DRE/DRF uncertainty

$$\boldsymbol{\sigma_{DRX}(t,i,j)} = \left[\left(\frac{\partial DRX}{\partial AOD} \Delta AOD - \frac{\partial DRX}{\partial SSA} \Delta SSA \right)^2 + \left(\frac{\partial DRX}{\partial g} \Delta g \right)^2 + \left(\frac{\partial DRX}{\partial a} \Delta a \right)^2 + \left(\frac{\partial DRX}{\partial COD} \Delta COD \right)^2 + \left(\frac{\partial DRF}{\partial f_{ant}} \Delta f_{ant} \right)^2 + \left(\sigma^z_{DRX} + \sigma^H_{DRX} + \sigma^\lambda_{DRX} \right)^2 \right]^{1/2}$$

- σ_{DRX}: total aerosol DRE/DRF uncertainty resolved for a single year every three hours (t) on a 2.5 degree grid (i, j) (will mostly focus on the global mean uncertainty)

Aerosol DRE/DRF uncertainty

$$\sigma_{DRX}(t,i,j) = \Bigg[\left(\frac{\partial \boldsymbol{DRX}}{\partial \boldsymbol{AOD}}\Delta AOD - \frac{\partial \boldsymbol{DRX}}{\partial \boldsymbol{SSA}}\Delta SSA\right)^2 + \left(\frac{\partial \boldsymbol{DRX}}{\partial \boldsymbol{g}}\Delta g\right)^2 + \left(\frac{\partial \boldsymbol{DRX}}{\partial \boldsymbol{a}}\Delta a\right)^2 + \left(\frac{\partial \boldsymbol{DRX}}{\partial \boldsymbol{COD}}\Delta COD\right)^2 + \left(\frac{\partial \boldsymbol{DRF}}{\partial \boldsymbol{f_{ant}}}\Delta f_{ant}\right)^2 + \left(\sigma^z_{DRX} + \sigma^H_{DRX} + \sigma^\lambda_{DRX}\right)^2\Bigg]^{1/2}$$

- σ_{DRX}: total aerosol DRE/DRF uncertainty resolved for a single year every three hours (t) on a 2.5 degree grid (i,j) (will mostly focus on the global mean uncertainty)
- $\partial DRX/\partial x$: DRE/DRF radiative kernels (Thorsen et al., 2020)

Aerosol DRE/DRF uncertainty

$$\sigma_{DRX}(t,i,j) = \Bigg[\left(\frac{\partial DRX}{\partial AOD}\boldsymbol{\Delta AOD} - \frac{\partial DRX}{\partial SSA}\boldsymbol{\Delta SSA}\right)^2 + \left(\frac{\partial DRX}{\partial g}\boldsymbol{\Delta g}\right)^2 + \left(\frac{\partial DRX}{\partial a}\Delta a\right)^2 + \left(\frac{\partial DRX}{\partial COD}\Delta COD\right)^2 + \left(\frac{\partial DRF}{\partial f_{ant}}\Delta f_{ant}\right)^2 + \left(\sigma^z_{DRX} + \sigma^H_{DRX} + \sigma^\lambda_{DRX}\right)^2\Bigg]^{1/2}$$

- σ_{DRX}: total aerosol DRE/DRF uncertainty resolved for a single year every three hours (t) on a 2.5 degree grid (i,j) (will mostly focus on the global mean uncertainty)
- $\partial DRX/\partial x$: DRE/DRF radiative kernels (Thorsen et al., 2020)
- Aerosol optical depth (AOD), single scattering albedo (SSA), asymmetry factor (g) [550nm]

Aerosol DRE/DRF uncertainty

$$\sigma_{DRX}(t,i,j) = \Bigg[\left(\frac{\partial DRX}{\partial AOD}\Delta AOD - \frac{\partial DRX}{\partial SSA}\Delta SSA\right)^2 + \left(\frac{\partial DRX}{\partial g}\Delta g\right)^2 + \left(\frac{\partial DRX}{\partial a}\boldsymbol{\Delta a}\right)^2 + \left(\frac{\partial DRX}{\partial COD}\boldsymbol{\Delta COD}\right)^2 + \left(\frac{\partial DRF}{\partial f_{ant}}\boldsymbol{\Delta f_{ant}}\right)^2 + \left(\sigma^z_{DRX} + \sigma^H_{DRX} + \sigma^\lambda_{DRX}\right)^2\Bigg]^{1/2}$$

- σ_{DRX}: total aerosol DRE/DRF uncertainty resolved for a single year every three hours (t) on a 2.5 degree grid (i,j) (will mostly focus on the global mean uncertainty)
- $\partial DRX/\partial x$: DRE/DRF radiative kernels (Thorsen et al., 2020)
- Aerosol optical depth (AOD), single scattering albedo (SSA), asymmetry factor (g) [550nm]
- Surface albedo (a), cloud optical depth (COD), and anthropogenic fraction (f_{ant})

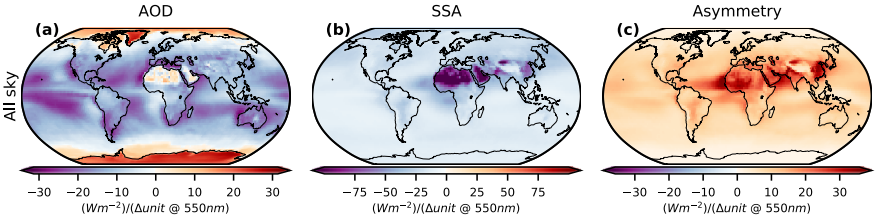
Aerosol DRE/DRF uncertainty

$$\sigma_{DRX}(t,i,j) = \Bigg[\left(\frac{\partial DRX}{\partial AOD}\Delta AOD - \frac{\partial DRX}{\partial SSA}\Delta SSA\right)^2 + \left(\frac{\partial DRX}{\partial g}\Delta g\right)^2 + \left(\frac{\partial DRX}{\partial a}\Delta a\right)^2 + \left(\frac{\partial DRX}{\partial COD}\Delta COD\right)^2 + \left(\frac{\partial DRF}{\partial f_{ant}}\Delta f_{ant}\right)^2 + \left(\boldsymbol{\sigma^z_{DRX}} + \boldsymbol{\sigma^H_{DRX}} + \boldsymbol{\sigma^\lambda_{DRX}}\right)^2\Bigg]^{1/2}$$

- σ_{DRX}: total aerosol DRE/DRF uncertainty resolved for a single year every three hours (t) on a 2.5 degree grid (i,j) (will mostly focus on the global mean uncertainty)
- $\partial DRX/\partial x$: DRE/DRF radiative kernels (Thorsen et al., 2020)
- Aerosol optical depth (AOD), single scattering albedo (SSA), asymmetry factor (g) [550nm]
- Surface albedo (a), cloud optical depth (COD), and anthropogenic fraction (f_{ant})
- Uncertainty from:
  - simplifications to the aerosol vertical profiles (σ^z_{DRX})
  - errors in the retrieval of aerosol scale height (σ^H_{DRX})
  - incomplete knowledge of spectral dependencies of the aerosol scattering properties (σ^λ_{DRX})

Kernels ($\partial DRX/\partial x$)

- Thorsen et al. (2020a): derived gridded (2.5 degree) three-hourly DRE kernels from 1 year of MERRA-2 data by imposing small perturbations to the base-state values of the aerosol scattering properties, surface albedo, and cloud properties
- Linearization of the radiation transfer calculations / useful for error propagation



- AOD kernel: mostly negative (i.e. cooling), but also can be positive in regions with high surface albedo (increased absorption).
- DRF kernels derived by applying the DRE kernels to AeroCom Phase II model simulations of PD and PI aerosol optical properties

DRF Kernels ($\partial DRF/\partial x$)

- $\mathrm{DRF}_{\mathrm{CLI}}$ radiative kernel can be approximated as a scaled DRE kernel:

$$\frac{\partial DRF_{CLI}}{\partial x} = \frac{\partial DRE}{\partial x} \times \left(\frac{DRF^{'}_{CLI}}{DRE^{'}} \right)$$

  - Scaled by the fraction of the radiative effect that is anthropogenic
- $DRF^{'}_{CLI}$ determined by applying the DRE kernels to AeroCom Phase II model simulations of PD and PI aerosol properties:

$$DRF^{'}_{CLI} \approx DRF^{k}_{CLI} = \frac{\partial DRE}{\partial AOD}\overline{(AOD_{PD} - AOD_{PI})} + \frac{\partial DRE}{\partial SSA}\overline{(SSA_{PD} - SSA_{PI})} + \frac{\partial DRE}{\partial g}\overline{(g_{PD} - g_{PI})}$$

  - Overbars: monthly, gridded, multi-model mean
- $DRE^{'}$: MERRA-2 based calculations in Thorsen et al. (2020a)

DRF Kernels ($\partial DRF/\partial x$)

$$DRF^{k}_{CLI} = \frac{\partial DRE}{\partial AOD}\overline{(AOD_{PD} - AOD_{PI})} + \frac{\partial DRE}{\partial SSA}\overline{(SSA_{PD} - SSA_{PI})} + \frac{\partial DRE}{\partial g}\overline{(g_{PD} - g_{PI})}$$

$$\frac{\partial DRF_{CLI}}{\partial x} = \frac{\partial DRE}{\partial x} \times \left(\frac{DRF^{k}_{CLI}}{DRE'}\right)$$

- Why do this when DRF is already archived in AeroCom? (Myhre et al., 2013)
  - Only a few models archive DRE
  - Would require dividing monthly averages of two non-linear quantities
  - AeroCom models contain differences due to uncertainties in non-aerosol properties such as clouds and surface albedo— so-called "host-model" uncertainties (Stier et al., 2013)

Model	DRF_{CLI}	DRF^{k}_{CLI}
CAM4-Oslo	-0.08	-0.21
CAM5.1	-0.02	-0.11
ECHAM5-HAM	-0.15	-0.21
GISS-MATRIX	-0.58	-0.34
GMI	-0.52	-0.45
GOCART	-0.36	-0.24
HadGEM2	-0.31	-0.27
IMPACT	-0.21	-0.53
OsloCTM2	-0.17	-0.25
SPRINTARS	-0.14	-0.23
TM5	-0.32	-0.16
Mean	**-0.26**	**-0.27**
Standard deviation	**0.17**	**0.12**

- Standard deviation reduced by approximating the DRF using kernels

Observational uncertainties: SSA/g

- For each of the three-hourly gridded data points in the MERRA-2 data, select a representative AERONET SSA and asymmetry factor uncertainty

Observational uncertainties: SSA/g

- For each of the three-hourly gridded data points in the MERRA-2 data, select a representative AERONET SSA and asymmetry factor uncertainty
  1. Define aerosol "type" vectors for AERONET and MERRA-2:

$$\overrightarrow{type} = (AOD^{\lambda_i}, AOD^{\lambda_i}_{fine}, AOD^{\lambda_i}_{coarse}, SSA^{\lambda_i}, g^{\lambda_i})$$

$$\lambda_i = \{440nm, 675nm, 870nm, 1020nm\}$$

Observational uncertainties: SSA/g

- For each of the three-hourly gridded data points in the MERRA-2 data, select a representative AERONET SSA and asymmetry factor uncertainty
  1. Define aerosol "type" vectors for AERONET and MERRA-2:

$$\overrightarrow{type} = (AOD^{\lambda_i}, AOD^{\lambda_i}_{fine}, AOD^{\lambda_i}_{coarse}, SSA^{\lambda_i}, g^{\lambda_i})$$

$$\lambda_i = \{440nm, 675nm, 870nm, 1020nm\}$$

  2. Find closest matching pair between AERONET/MERRA-2 $\overrightarrow{type}$ (i.e. minimize the standardized Euclidean distance)
     - Use entire AERONET database from 2000-2019 (20 years)
     - Typically, a close match is found: median differences in the 20 optical properties $< 6\%$

Observational uncertainties: SSA/g

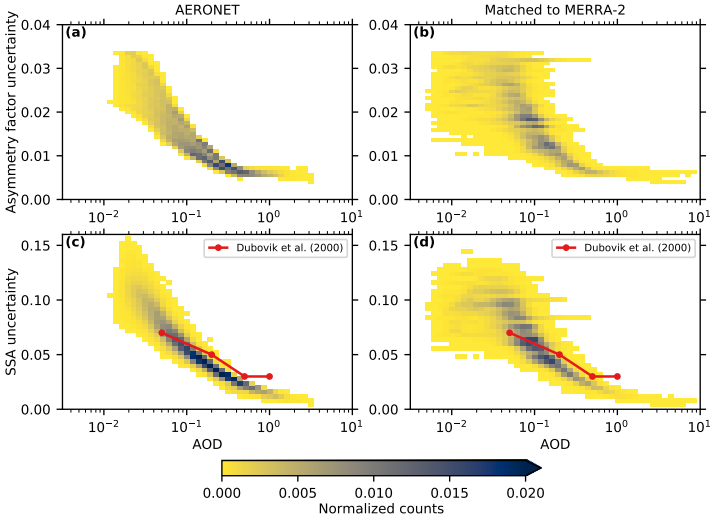
- For each of the three-hourly gridded data points in the MERRA-2 data, select a representative AERONET SSA and asymmetry factor uncertainty
  1. Define aerosol "type" vectors for AERONET and MERRA-2:

$$\overrightarrow{type} = (AOD^{\lambda_i}, AOD^{\lambda_i}_{fine}, AOD^{\lambda_i}_{coarse}, SSA^{\lambda_i}, g^{\lambda_i})$$

$$\lambda_i = \{440nm, 675nm, 870nm, 1020nm\}$$

  2. Find closest matching pair between AERONET/MERRA-2 $\overrightarrow{type}$ (i.e. minimize the standardized Euclidean distance)
     - Use entire AERONET database from 2000-2019 (20 years)
     - Typically, a close match is found: median differences in the 20 optical properties $< 6\%$
  3. For the matching AERONET observation, take ΔSSA, Δg from the AERONET aerosol inversion uncertainty data product ("U27" product)

Observational uncertainties: aerosol optical properties



- **Left**: Δg, ΔSSA from U27 AERONET product (2000-2019)
- **Right**: after matches are made to the MERRA-2 data points
  - Strong dependence on AOD since information content decreases with decreasing AOD

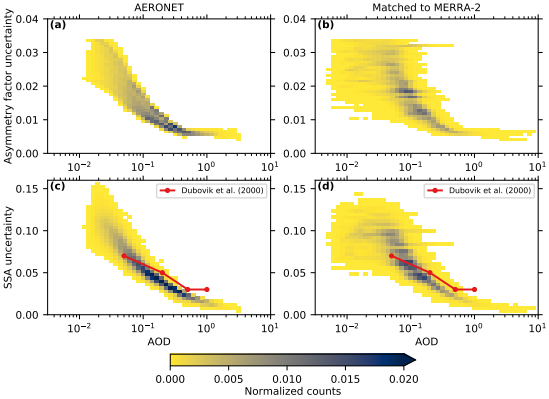
Observational uncertainties: SSA/g

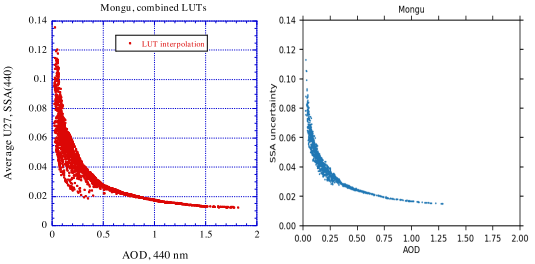
- For each of the three-hourly gridded data points in the MERRA-2 data, select a representative AERONET SSA and asymmetry factor uncertainty
- Find matching pairs of aerosol "type" vectors for AERONET/MERRA-2:

$$\overrightarrow{type} = (AOD^{\lambda_i}, AOD^{\lambda_i}_{fine}, AOD^{\lambda_i}_{coarse}, SSA^{\lambda_i}, g^{\lambda_i})$$

$$\lambda_i = \{440nm, 675nm, 870nm, 1020nm\}$$

- AERONET U27: SSA uncertainty only provided when AOD$\geq$0.4 $\rightarrow$ multiple linear regression used get SSA uncertainty at smaller AODs
  - Predictors: $\overrightarrow{type}$, ΔG, fine/coarse mode volume median radius uncertainty, fine/coarse mode size distribution width uncertainty, and the sun and sky residual errors.
  - Regression coefficients are used to calculate ΔSSA when $AOD < 0.4$
  - $r^2 = 0.87$–0.96 (depending on the month)





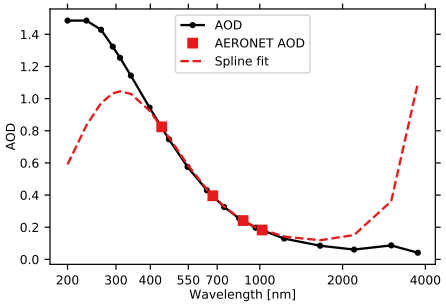
Observational uncertainties: Other properties

MODIS-based uncertainties taken from literature:

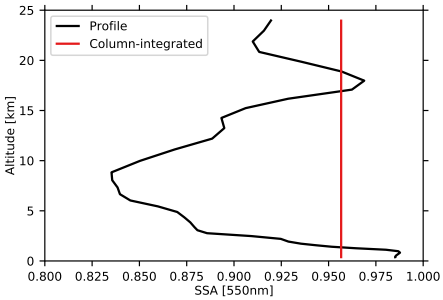
- Land surface albedo uncertainty = 0.02: about the agreement between the MODIS BRDF Albedo product (MCD43) and surface stations measurements
  (Jin et al., 2003; Cescatti et al., 2012; Roman et al., 2013; Stroeve et al., 2013; Wang et al., 2014)
- Ocean surface albedo uncertainty = 8%: comparison of Jin et al. (2004) parameterization to observations (Jin et al., 2005)
- Cloud optical depth uncertainty = 25% (Grosvenor et al., 2018)
- Anthropogenic fraction = 30% (Kaufman et al., 2005)

Observational uncertainties: vertical/spectral simplifications

- To compute the aerosol DRE/DRF, the aerosol optical properties need to be specified in each vertical layer (72) and across the broadband spectrum (175nm-4μm)
- AERONET sun photometers only retrieve **column-averaged** aerosol scattering properties at **limited wavelengths** (440, 675, 870, 1020 nm)
- Compute impact: kernels + take MERRA-2 vertical/spectral properties as "truth" (assumed to be representative of 1σ systematic uncertainty)



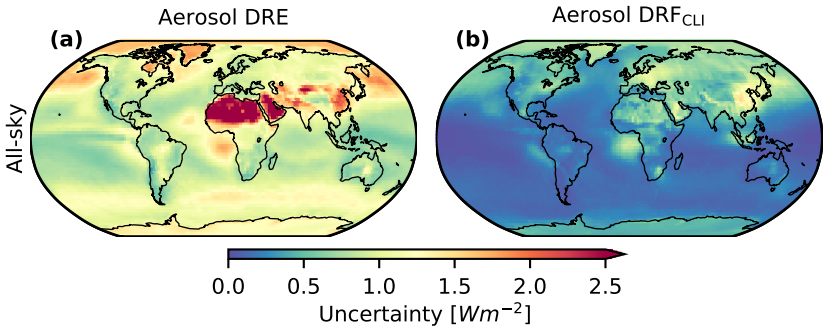
- Use the limited set of wavelengths to interpolate/extrapolate to the broadband



- (Column-Averaged) minus (Full Profile)
- Full extinction profile simplified into an AOD and a scale height: $\exp(-z/H)$
- Uncertainty in the scale height = 900m

(Waquet et al., 2009; Wu et al., 2016)

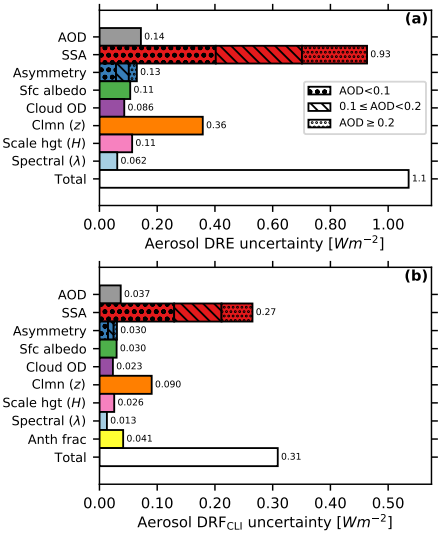
DRE/DRF regional uncertainty



- DRE uncertainty is largest in regions dominated by dust
- DRF uncertainty much smaller than DRE, particularly over ocean. Largest uncertainties over Northern Hemisphere land

Reducing observational uncertainties

- Current (optimistic) observational uncertainty for the approach of using observed optical properties to forward model the aerosol DRE/DRF
- How to reduce this uncertainty?
  1. Total uncertainty dominated by the SSA, particularly when the AOD is smaller (AOD<0.2)
  2. Next largest contributer: use of column-averaged aerosol optical properties
- Explore an "enhanced" approach that addresses ❶+❷



Reducing observational uncertainties

$$\sigma_{DRX} = \Bigg[\left(\frac{\partial DRX}{\partial AOD} \Delta AOD - \frac{\partial DRX}{\partial SSA} \Delta SSA \right)^2 + \left(\frac{\partial DRX}{\partial g} \Delta g \right)^2 + \left(\frac{\partial DRX}{\partial a} \Delta a \right)^2 + \left(\frac{\partial DRX}{\partial COD} \Delta COD \right)^2 + \left(\frac{\partial DRF}{\partial f_{ant}} \Delta f_{ant} \right)^2 + \left(\sigma^z_{DRX} + \sigma^H_{DRX} + \sigma^\lambda_{DRX} \right)^2 \Bigg]^{1/2}$$

❶ Avoid using SSA at low AODs:

- Instead of using directly-retrieved SSAs, an identification of aerosol type (e.g. dust, sea salt, etc) could be made and the optical properties taken from pre-determined optical model
  - Satellite aerosol typing algorithms (e.g. Omar et al., 2009; Russell et al., 2014; Kahn and Gaitley, 2015; Kim et al., 2018) have a limited ability to identify mixtures of aerosol types (Burton et al., 2013; Nowottnick et al., 2015) compared to more advanced ground-based/airborne remote sensors (Burton et al., 2014)

- Hypothetical capability that can perfectly identify any mixture of the MERRA-2 aerosols (dust, sea salt, sulfate, black and organic carbon)
- Directly-retrieved SSA is only used for absorbing aerosol types (dust, black and organic carbon)
- For sea salt and sulfate, assume that the SSA is known perfectly (i.e. ~ 1.0 at visible wavelengths)

Reducing observational uncertainties

$$\sigma_{DRX} = \Bigg[\left(\frac{\partial DRX}{\partial AOD} \Delta AOD - \boldsymbol{\frac{\partial DRX}{\partial SSA}} \Delta SSA \right)^2 + \left(\frac{\partial DRX}{\partial g} \Delta g \right)^2 + \left(\frac{\partial DRX}{\partial a} \Delta a \right)^2 + \left(\frac{\partial DRX}{\partial COD} \Delta COD \right)^2 + \left(\frac{\partial DRF}{\partial f_{ant}} \Delta f_{ant} \right)^2 + \left(\sigma^z_{DRX} + \sigma^H_{DRX} + \sigma^\lambda_{DRX} \right)^2 \Bigg]^{1/2}$$

❶ Avoid using SSA at low AODs:

- Instead of using directly-retrieved SSAs, an identification of aerosol type (e.g. dust, sea salt, etc) could be made and the optical properties taken from pre-determined optical model
  - Satellite aerosol typing algorithms (e.g. Omar et al., 2009; Russell et al., 2014; Kahn and Gaitley, 2015; Kim et al., 2018) have a limited ability to identify mixtures of aerosol types (Burton et al., 2013; Nowottnick et al., 2015) compared to more advanced ground-based/airborne remote sensors (Burton et al., 2014)

- Hypothetical capability that can perfectly identify any mixture of the MERRA-2 aerosols (dust, sea salt, sulfate, black and organic carbon)
- Directly-retrieved SSA is only used for absorbing aerosol types (dust, black and organic carbon)
- For sea salt and sulfate, assume that the SSA is known perfectly (i.e. ~ 1.0 at visible wavelengths)

Reducing observational uncertainties

$$\sigma_{DRX} = \Bigg[\left(\frac{\partial DRX}{\partial AOD} \Delta AOD - \boldsymbol{\frac{\partial DRX}{\partial SSA_{abs}}} \Delta SSA \right)^2 + \left(\frac{\partial DRX}{\partial g} \Delta g \right)^2 + \left(\frac{\partial DRX}{\partial a} \Delta a \right)^2 + \left(\frac{\partial DRX}{\partial COD} \Delta COD \right)^2 + \left(\frac{\partial DRF}{\partial f_{ant}} \Delta f_{ant} \right)^2 + \left(\sigma^z_{DRX} + \sigma^H_{DRX} + \sigma^\lambda_{DRX} \right)^2 \Bigg]^{1/2}$$

❶ Avoid using SSA at low AODs:

- Instead of using directly-retrieved SSAs, an identification of aerosol type (e.g. dust, sea salt, etc) could be made and the optical properties taken from pre-determined optical model
  - Satellite aerosol typing algorithms (e.g. Omar et al., 2009; Russell et al., 2014; Kahn and Gaitley, 2015; Kim et al., 2018) have a limited ability to identify mixtures of aerosol types (Burton et al., 2013; Nowottnick et al., 2015) compared to more advanced ground-based/airborne remote sensors (Burton et al., 2014)

- Hypothetical capability that can perfectly identify any mixture of the MERRA-2 aerosols (dust, sea salt, sulfate, black and organic carbon)
- Directly-retrieved SSA is only used for absorbing aerosol types (dust, black and organic carbon)
- For sea salt and sulfate, assume that the SSA is known perfectly (i.e. ~ 1.0 at visible wavelengths)

Reducing observational uncertainties

$$\sigma_{DRX} = \left[\left(\frac{\partial DRX}{\partial AOD} \Delta AOD - \frac{\partial DRX}{\partial SSA_{abs}} \Delta SSA \right)^2 + \left(\frac{\partial DRX}{\partial g} \Delta g \right)^2 + \left(\frac{\partial DRX}{\partial a} \Delta a \right)^2 + \left(\frac{\partial DRX}{\partial COD} \Delta COD \right)^2 + \left(\frac{\partial DRF}{\partial f_{ant}} \Delta f_{ant} \right)^2 + \left(\boldsymbol{\sigma^{z}_{DRX}} + \boldsymbol{\sigma^{H}_{DRX}} + \sigma^{\lambda}_{DRX} \right)^2 \right]^{1/2}$$

❷ Improve vertical representation with lidar:

- Potential to provide highly accurate extinction profiles at a fine vertical resolution (e.g. Thorsen and Fu, 2015a; Hair et al., 2008)
- Ability to provide vertically-resolved microphysical properties (i.e. SSA and asymmetry factor) is more limited (Burton et al., 2016)
  - Combined lidar+polarimeter retrieval techniques to obtain these aerosol microphysical properties is an emerging area of research (Knobelspiesse et al., 2011; Lopatin et al., 2013; Chaikovsky et al., 2016; Stamnes et al., 2018),
    but the accuracies of these approaches are not yet well established

---

- Assume a lidar-provided extinction profile eliminates the need for the aerosol scale height
- Assume a hypothetical capability to retrieve optical properties (AOD, SSA and asymmetry factor) in 2 layers: the planetary boundary layer (PBL) and the free troposphere (FT)

Reducing observational uncertainties

$$\sigma_{DRX} = \left[\left(\frac{\partial DRX}{\partial AOD} \Delta AOD - \frac{\partial DRX}{\partial SSA_{abs}} \Delta SSA \right)^2 + \left(\frac{\partial DRX}{\partial g} \Delta g \right)^2 + \left(\frac{\partial DRX}{\partial a} \Delta a \right)^2 + \left(\frac{\partial DRX}{\partial COD} \Delta COD \right)^2 + \left(\frac{\partial DRF}{\partial f_{ant}} \Delta f_{ant} \right)^2 + \left(\sigma_{DRX}^{z,2lyr} + \cancel{\sigma_{DRX}^{H}} + \sigma_{DRX}^{\lambda} \right)^2 \right]^{1/2}$$

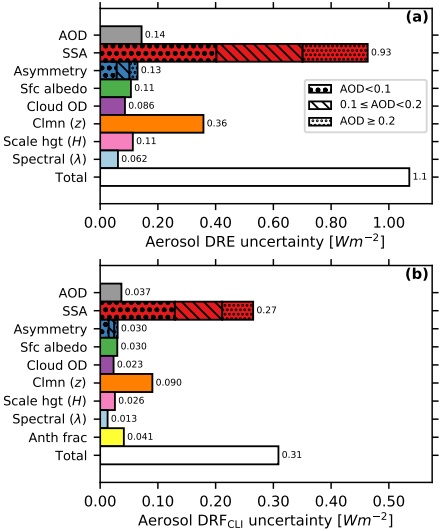
❷ Improve vertical representation with lidar:

- Potential to provide highly accurate extinction profiles at a fine vertical resolution (e.g. Thorsen and Fu, 2015a; Hair et al., 2008)
- Ability to provide vertically-resolved microphysical properties (i.e. SSA and asymmetry factor) is more limited (Burton et al., 2016)
  - Combined lidar+polarimeter retrieval techniques to obtain these aerosol microphysical properties is an emerging area of research (Knobelspiesse et al., 2011; Lopatin et al., 2013; Chaikovsky et al., 2016; Stamnes et al., 2018),
    but the accuracies of these approaches are not yet well established

---

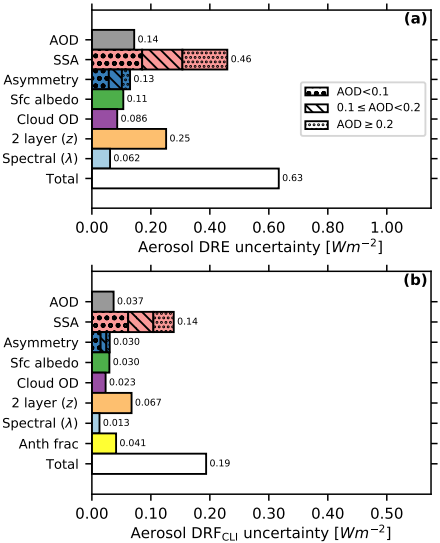
- Assume a lidar-provided extinction profile eliminates the need for the aerosol scale height
- Assume a hypothetical capability to retrieve optical properties (AOD, SSA and asymmetry factor) in 2 layers: the planetary boundary layer (PBL) and the free troposphere (FT)

Re-assessed DRE/DRF uncertainty



$$\sigma_{DRX} = \left[\left(\frac{\partial DRX}{\partial AOD} \Delta AOD - \frac{\boldsymbol{\partial DRX}}{\boldsymbol{\partial SSA_{abs}}} \Delta SSA \right)^2 + \left(\frac{\partial DRX}{\partial g} \Delta g \right)^2 + \left(\frac{\partial DRX}{\partial a} \Delta a \right)^2 + \left(\frac{\partial DRX}{\partial COD} \Delta COD \right)^2 + \left(\frac{\partial DRF}{\partial f_{ant}} \Delta f_{ant} \right)^2 + \left(\boldsymbol{\sigma_{DRX}^{z,2lyr}} + \cancel{\boldsymbol{\sigma_{DRX}^{H}}} + \sigma_{DRX}^{\lambda} \right)^2 \right]^{1/2}$$

Re-assessed DRE/DRF uncertainty



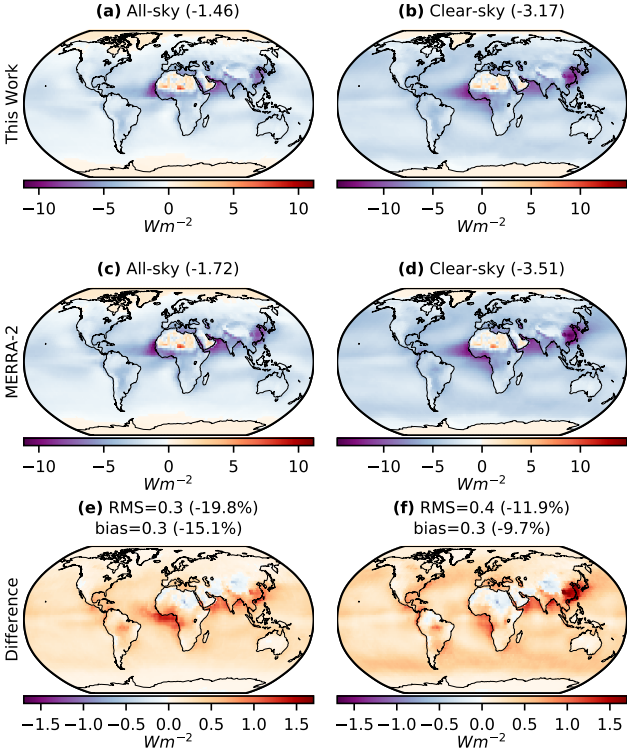
$$\sigma_{DRX} = \left[\left(\frac{\partial DRX}{\partial AOD}\Delta AOD - \frac{\partial DRX}{\partial SSA_{abs}}\Delta SSA\right)^2 + \left(\frac{\partial DRX}{\partial g}\Delta g\right)^2 + \left(\frac{\partial DRX}{\partial a}\Delta a\right)^2 + \left(\frac{\partial DRX}{\partial COD}\Delta COD\right)^2 + \left(\frac{\partial DRF}{\partial f_{ant}}\Delta f_{ant}\right)^2 + \left(\sigma_{DRX}^{z,2lyr} + \cancel{\sigma_{DRX}^{H}} + \sigma_{DRX}^{\lambda}\right)^2\right]^{1/2}$$

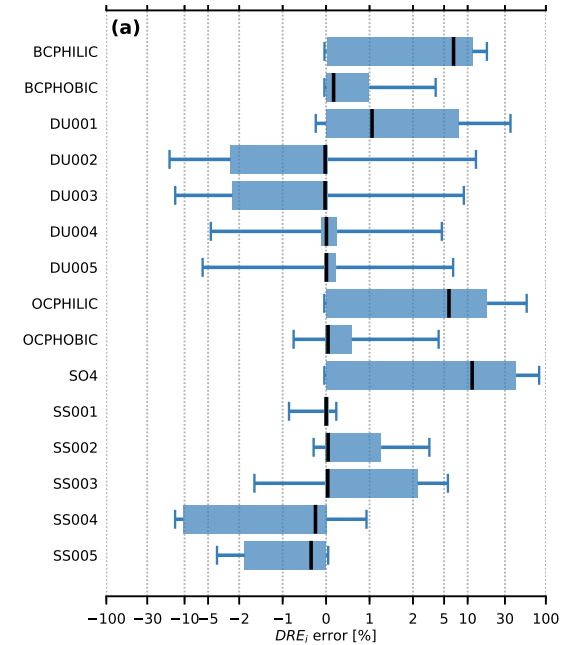
- SSA uncertainty only from absorbing aerosols, the extinction profile is measured, 2 layers (the PBL and FT) of aerosol scattering properties are retrieved
- Compared to original assessment, total uncertainty is reduced by ∼40%

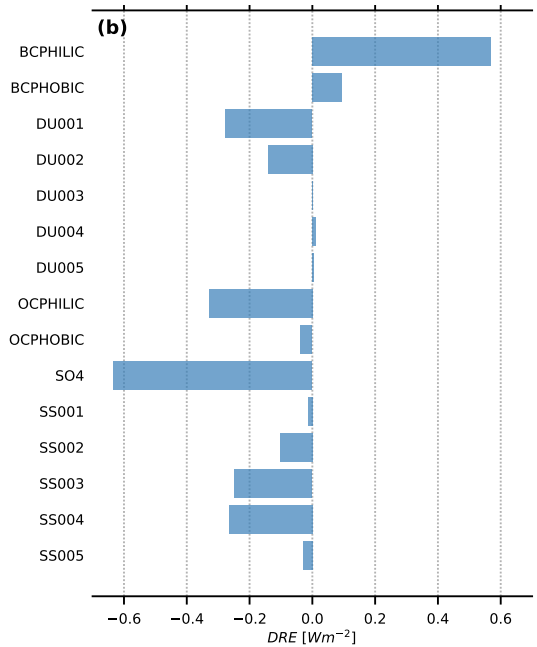
Collection	Variables	Description
inst3_3d_asm_Nv	T	temperature
	QV	specific humidity
	O3	ozone
	CLOUD	cloud fraction
tavg1_2d_rad_Nx	ALBVISDR, ALBVISDF	direct, diffuse visible surface albedo
	ALBNIRDR, ALBNIRDF	direct, diffuse near infrared surface albedo
	CLDLOW, CLDMID, CLDHGH	low, middle, high cloud super-layer area fraction
	TAULOW, TAUMID, TAUHGH	low, middle, high cloud super-layer optical depth
tavg3_3d_cld_Nv	TAUCLW, TAUCLI	liquid, ice cloud optical depth
	INCLOUDQL, INCLOUDQI	liquid, ice cloud mass mixing ratio
inst3_3d_aer_Nv	RH	relative humidity
	AIRDENS	air density
	DU001, DU002, DU003, DU004, DU005	Dust mass mixing ratio, bins 1–5
	SS001, SS002, SS003, SS004, SS005	Sea salt mass mixing ratio, bins 1–5
	SO4	Sulphate mass mixing ratio
	BCPHOBIC, BCPHILIC	Hydrophobic, hydrophilic black carbon mass mixing ratio
	OCPHOBIC, OCPHILIC	Hydrophobic, hydrophilic organic carbon mass mixing ratio

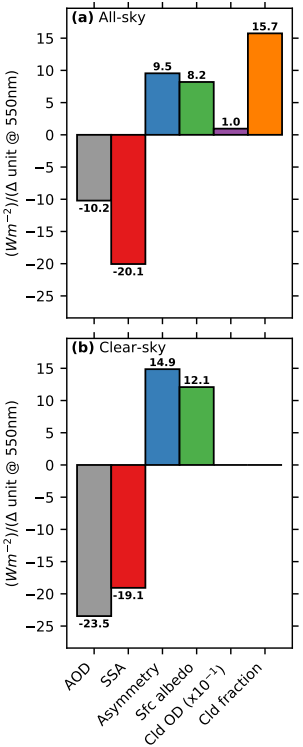
	RMS error		Bias error	
	All-sky	Clear-sky	All-sky	Clear-sky
This study	15.4	4.3	-3.5	1.0
MERRA-2	15.3	4.3	-6.2	2.0

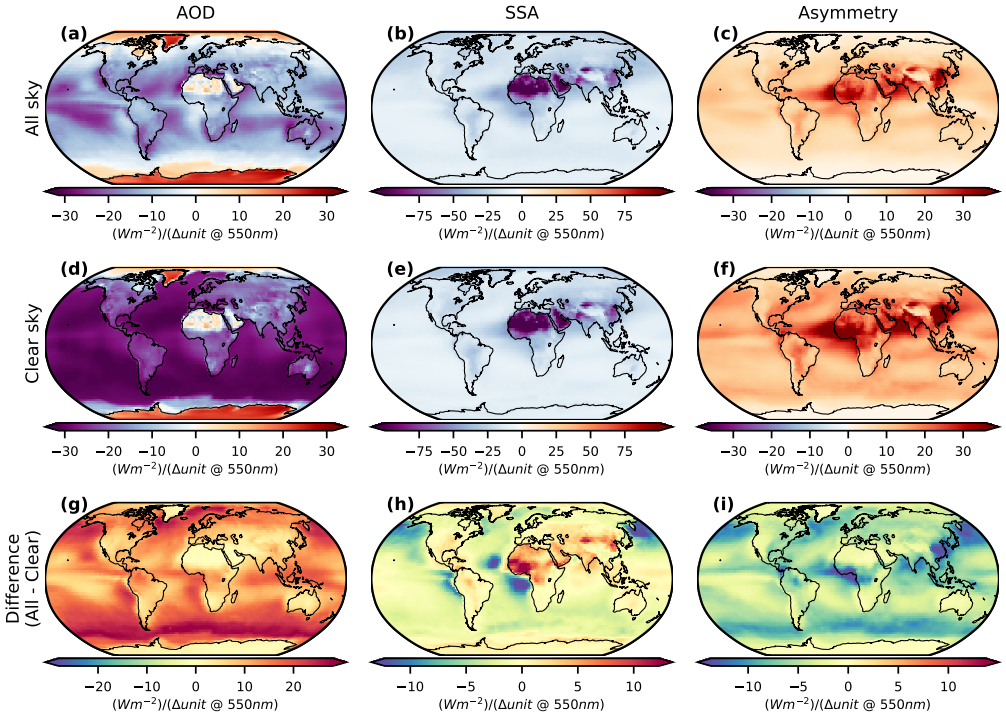
Band number	Wavelength range (μm)
1	0.1754–0.2247
2	0.2247–0.2439
3	0.2439–0.2857
4	0.2857–0.2985
5	0.2985–0.3225
6	0.3225–0.3575
7	0.3575–0.4375
8	0.4375–0.4975
9	0.4975–0.595
10	0.595–0.6896
11	0.690–0.794
12	0.794–0.889
13	0.889–1.042
14	1.042–1.410
15	1.410–1.9048
16	1.9048–2.5
17	2.5–3.5088
18	3.5088–4

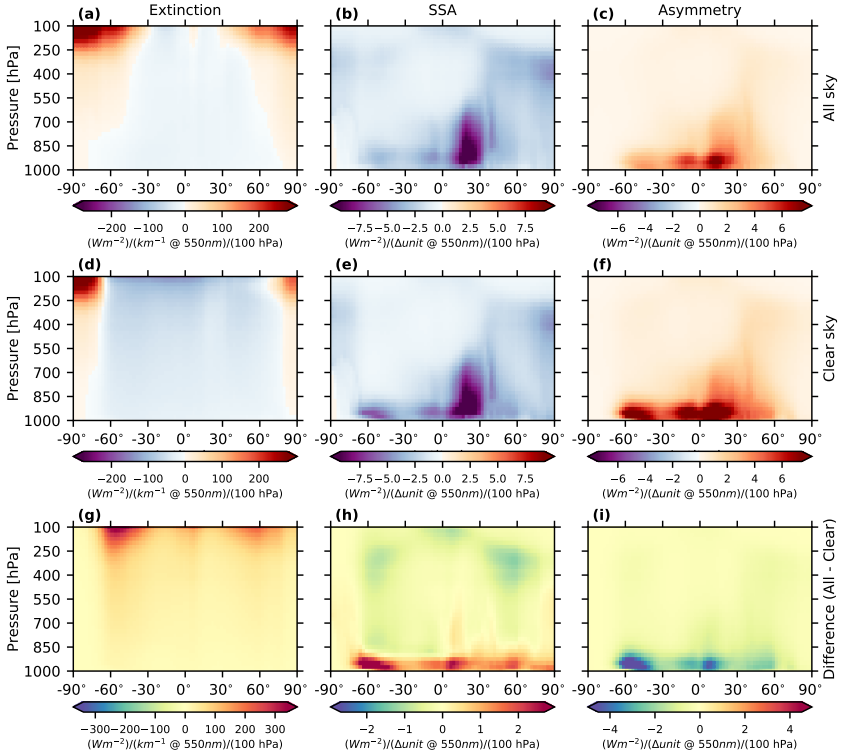

(a) All-sky (-1.46)
(b) Clear-sky (-3.17)
This Work
−10 −5 0 5 10
Wm^{-2}
(c) All-sky (-1.72)
(d) Clear-sky (-3.51)
MERRA-2
(e) RMS=0.3 (-19.8%)
bias=0.3 (-15.1%)
(f) RMS=0.4 (-11.9%)
bias=0.3 (-9.7%)
Difference
−1.5 −1.0 −0.5 0.0 0.5 1.0 1.5

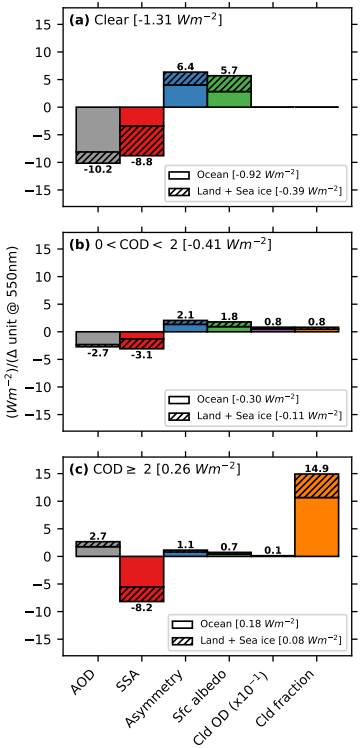

(a)
BCPHILIC
BCPHOBIC
DU001
DU002
DU003
DU004
DU005
OCPHILIC
OCPHOBIC
SO4
SS001
SS002
SS003
SS004
SS005
−100 −30 −10 −5 −2 −1 0 1 2 5 10 30 100
DRE$_i$ error [%]

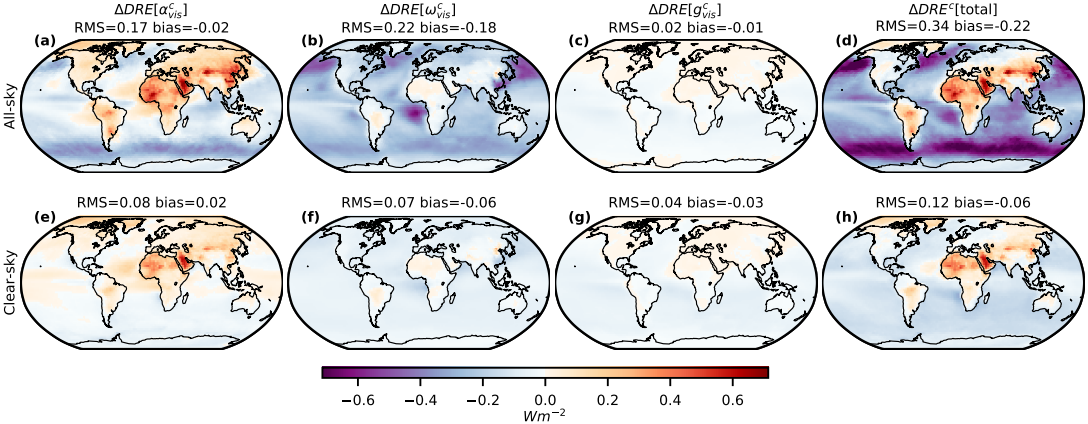

(b)
BCPHILIC
BCPHOBIC
DU001
DU002
DU003
DU004
DU005
OCPHILIC
OCPHOBIC
SO4
SS001
SS002
SS003
SS004
SS005
−0.6 −0.4 −0.2 0.0 0.2 0.4 0.6
DRE [Wm^{-2}]

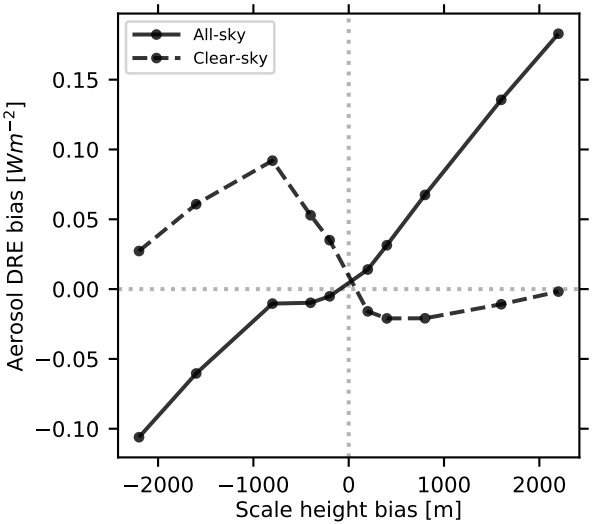

(a) All-sky
(b) Clear-sky
(Wm^{-2})/(Δ unit @ 550nm)
-10.2
-20.1
9.5
8.2
1.0
15.7
-23.5
-19.1
14.9
12.1
AOD
SSA
Asymmetry
Sfc albedo
Cld OD (x10^{-1})
Cld fraction

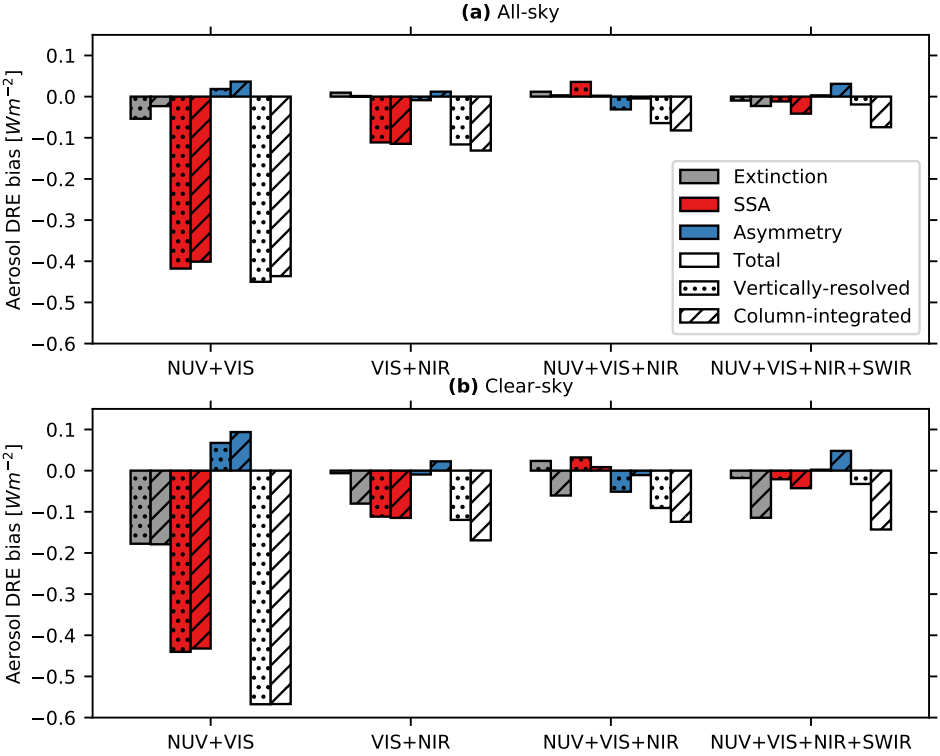

AOD
SSA
Asymmetry
(a)
(b)
(c)
All sky
−30 −20 −10 0 10 20 30
−75 −50 −25 0 25 50 75
−30 −20 −10 0 10 20 30
$(Wm^{-2})/(\Delta unit\ @\ 550nm)$
(d)
(e)
(f)
Clear sky
−30 −20 −10 0 10 20 30
−75 −50 −25 0 25 50 75
−30 −20 −10 0 10 20 30
$(Wm^{-2})/(\Delta unit\ @\ 550nm)$
(g)
(h)
(i)
Difference (All - Clear)
−20 −10 0 10 20
−10 −5 0 5 10
−10 −5 0 5 10
$(Wm^{-2})/(\Delta unit\ @\ 550nm)$


(a)
Extinction
(b)
SSA
(c)
Asymmetry
All sky
(d)
(e)
(f)
Clear sky
(g)
(h)
(i)
Difference (All - Clear)
Pressure [hPa]
100
250
400
550
700
850
1000
-90° -60° -30° 0° 30° 60° 90°
−200 −100 0 100 200
(Wm⁻²)/(km⁻¹ @ 550nm)/(100 hPa)
−7.5 −5.0 −2.5 0.0 2.5 5.0 7.5
(Wm⁻²)/(Δunit @ 550nm)/(100 hPa)
−6 −4 −2 0 2 4 6
(Wm⁻²)/(Δunit @ 550nm)/(100 hPa)
−300 −200 −100 0 100 200 300
(Wm⁻²)/(km⁻¹ @ 550nm)/(100 hPa)
−2 −1 0 1 2
(Wm⁻²)/(Δunit @ 550nm)/(100 hPa)
−4 −2 0 2 4
(Wm⁻²)/(Δunit @ 550nm)/(100 hPa)


(a) Clear [-1.31 Wm^{-2}]
6.4
5.7
-10.2
-8.8
Ocean [-0.92 Wm^{-2}]
Land + Sea ice [-0.39 Wm^{-2}]
(b) 0 < COD < 2 [-0.41 Wm^{-2}]
2.1
1.8
0.8
0.8
-2.7
-3.1
Ocean [-0.30 Wm^{-2}]
Land + Sea ice [-0.11 Wm^{-2}]
(c) COD ≥ 2 [0.26 Wm^{-2}]
14.9
2.7
1.1
0.7
0.1
-8.2
Ocean [0.18 Wm^{-2}]
Land + Sea ice [0.08 Wm^{-2}]
(Wm^{-2})/(Δ unit @ 550nm)
AOD
SSA
Asymmetry
Sfc albedo
Cld OD (x10^{-1})
Cld fraction

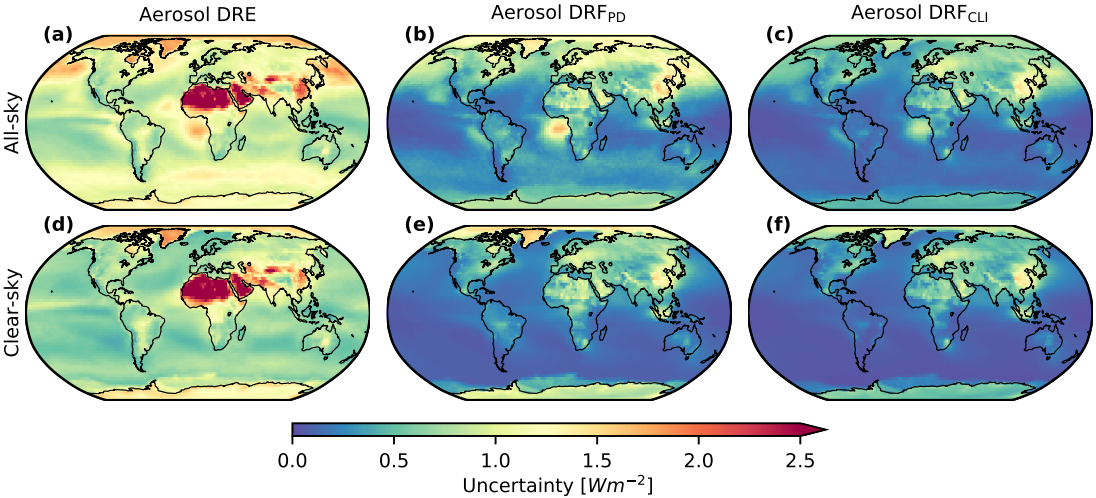

$\Delta DRE[\alpha^c_{vis}]$
RMS=0.17 bias=-0.02
(a)
$\Delta DRE[\omega^c_{vis}]$
RMS=0.22 bias=-0.18
(b)
$\Delta DRE[g^c_{vis}]$
RMS=0.02 bias=-0.01
(c)
ΔDRE^c[total]
RMS=0.34 bias=-0.22
(d)
All-sky
RMS=0.08 bias=0.02
(e)
RMS=0.07 bias=-0.06
(f)
RMS=0.04 bias=-0.03
(g)
RMS=0.12 bias=-0.06
(h)
Clear-sky
−0.6 −0.4 −0.2 0.0 0.2 0.4 0.6
Wm^{-2}

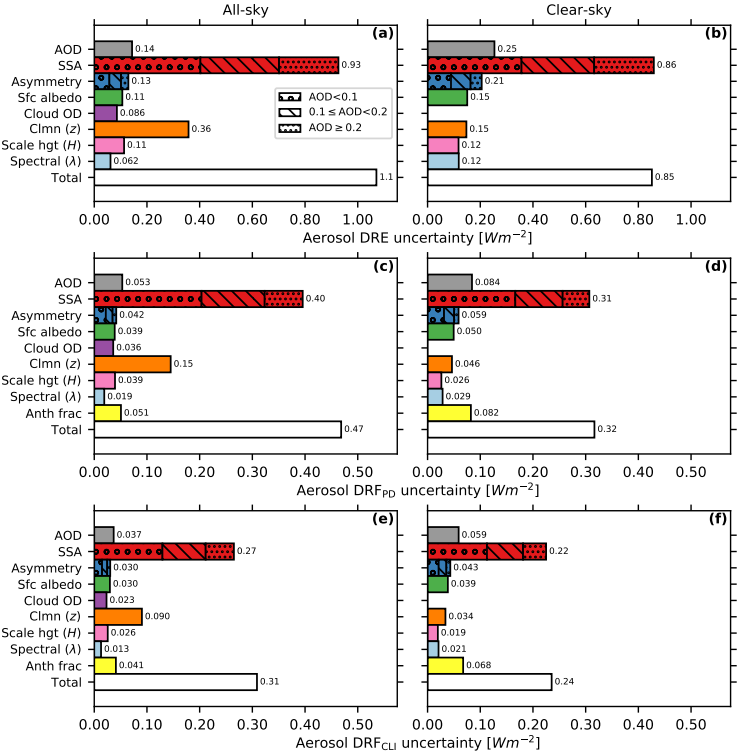

All-sky
Clear-sky
0.15
0.10
0.05
0.00
−0.05
−0.10
Aerosol DRE bias [Wm^{-2}]
−2000
−1000
0
1000
2000
Scale height bias [m]

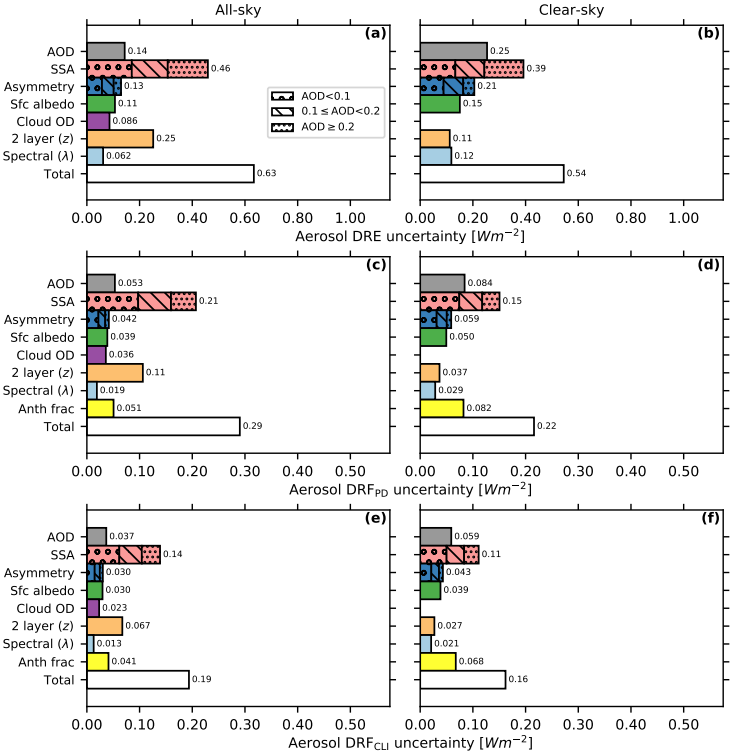

(a) All-sky
Aerosol DRE bias [Wm^{-2}]
0.1
0.0
−0.1
−0.2
−0.3
−0.4
−0.5
−0.6
Extinction
SSA
Asymmetry
Total
Vertically-resolved
Column-integrated
NUV+VIS
VIS+NIR
NUV+VIS+NIR
NUV+VIS+NIR+SWIR
(b) Clear-sky
Aerosol DRE bias [Wm^{-2}]
0.1
0.0
−0.1
−0.2
−0.3
−0.4
−0.5
−0.6
NUV+VIS
VIS+NIR
NUV+VIS+NIR
NUV+VIS+NIR+SWIR

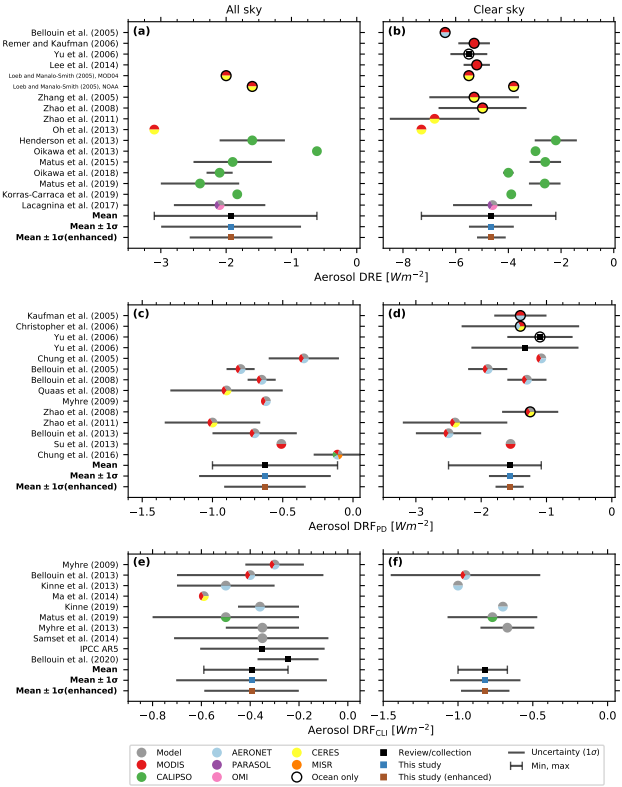
Model	Reference(s)	$(g_{PD} - g_{PI})$	$(AOD_{PI} - AOD_{PI_nat})$	$(SSA_{PI} - SSA_{PI_nat})$
CAM4-Oslo	Kirkevåg et al. (2012)	X	X	X
CAM5.1	Liu et al. (2012)		X	
ECHAM5-HAM	Vignati et al. (2004); Stier et al. (2005); Zhang et al. (2012)			
GISS-MATRIX	Bauer et al. (2008, 2010)	X		
GMI	Bian et al. (2009)	X	X	X
GOCART	Chin et al. (2000, 2002); Ginoux et al. (2001)	X	X	
HadGEM2	Bellouin et al. (2011)			
IMPACT	Wang and Penner (2009); Lin et al. (2012); Xu and Penner (2012)	X		
OsloCTM2	Myhre et al. (2007, 2009); Skeie et al. (2011)	X	X	
SPRINTARS	Takemura (2005); Takemura et al. (2009)		X	
TM5	Vignati et al. (2004); Aan de Brugh et al. (2011)	X	X	

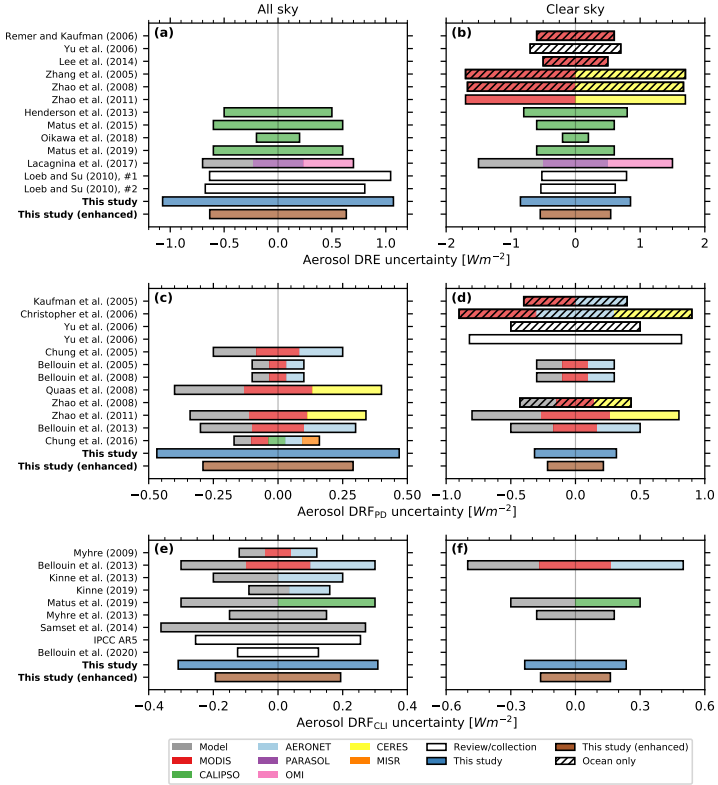
	All sky		Clear sky	
Model	DRF_{CLI}	DRF^{k}_{CLI}	DRF_{CLI}	DRF^{k}_{CLI}
CAM4-Oslo*	-0.08	-0.21		-0.87
CAM5.1	-0.02	-0.11	-0.35	-0.28
ECHAM5-HAM	-0.15	-0.21	-0.44	-0.58
GISS-MATRIX*	-0.58	-0.34	-0.79	-0.67
GMI*	-0.52	-0.45	-0.91	-0.90
GOCART*	-0.36	-0.24	-0.58	-0.57
HadGEM2	-0.31	-0.27	-0.72	-0.59
IMPACT*	-0.21	-0.53	-1.01	-1.06
OsloCTM2*	-0.17	-0.25	-0.69	-0.57
SPRINTARS	-0.14	-0.23	-0.71	-0.53
TM5*	-0.32	-0.16	-0.51	-0.34
Mean	-0.26	-0.27	-0.67	-0.63
Standard deviation	0.17	0.12	0.20	0.22


Aerosol DRE
Aerosol DRF$_{PD}$
Aerosol DRF$_{CLI}$
(a)
(b)
(c)
(d)
(e)
(f)
All-sky
Clear-sky
0.0
0.5
1.0
1.5
2.0
2.5
Uncertainty [Wm^{-2}]


All-sky
Clear-sky
(a)
(b)
(c)
(d)
(e)
(f)
AOD
SSA
Asymmetry
Sfc albedo
Cloud OD
Clmn (z)
Scale hgt (H)
Spectral (λ)
Anth frac
Total
AOD<0.1
0.1 ≤ AOD<0.2
AOD ≥ 0.2
0.14
0.93
0.13
0.11
0.086
0.36
0.11
0.062
1.1
0.25
0.86
0.21
0.15
0.15
0.12
0.12
0.85
0.053
0.40
0.042
0.039
0.036
0.15
0.039
0.019
0.051
0.47
0.084
0.31
0.059
0.050
0.046
0.026
0.029
0.082
0.32
0.037
0.27
0.030
0.030
0.023
0.090
0.026
0.013
0.041
0.31
0.059
0.22
0.043
0.039
0.034
0.019
0.021
0.068
0.24
0.00 0.20 0.40 0.60 0.80 1.00
Aerosol DRE uncertainty [Wm^{-2}]
0.00 0.10 0.20 0.30 0.40 0.50
Aerosol DRF_{PD} uncertainty [Wm^{-2}]
Aerosol DRF_{CLI} uncertainty [Wm^{-2}]


All-sky
Clear-sky
(a)
(b)
(c)
(d)
(e)
(f)
AOD
SSA
Asymmetry
Sfc albedo
Cloud OD
2 layer (z)
Spectral (λ)
Anth frac
Total
AOD<0.1
0.1 ≤ AOD<0.2
AOD ≥ 0.2
0.14
0.46
0.13
0.11
0.086
0.25
0.062
0.63
0.25
0.39
0.21
0.15
0.11
0.12
0.54
0.053
0.21
0.042
0.039
0.036
0.11
0.019
0.051
0.29
0.084
0.15
0.059
0.050
0.037
0.029
0.082
0.22
0.037
0.14
0.030
0.030
0.023
0.067
0.013
0.041
0.19
0.059
0.11
0.043
0.039
0.027
0.021
0.068
0.16
0.00 0.20 0.40 0.60 0.80 1.00
Aerosol DRE uncertainty [Wm^{-2}]
0.00 0.10 0.20 0.30 0.40 0.50
Aerosol DRF_{PD} uncertainty [Wm^{-2}]
Aerosol DRF_{CLI} uncertainty [Wm^{-2}]


All sky
Clear sky
(a)
(b)
Bellouin et al. (2005)
Remer and Kaufman (2006)
Yu et al. (2006)
Lee et al. (2014)
Loeb and Manalo-Smith (2005), MODO4
Loeb and Manalo-Smith (2005), NOAA
Zhang et al. (2005)
Zhao et al. (2008)
Zhao et al. (2011)
Oh et al. (2013)
Henderson et al. (2013)
Oikawa et al. (2013)
Matus et al. (2015)
Oikawa et al. (2018)
Matus et al. (2019)
Korras-Carraca et al. (2019)
Lacagnina et al. (2017)
Mean
Mean ± 1σ
Mean ± 1σ(enhanced)
−3 −2 −1 0
−8 −6 −4 −2 0
Aerosol DRE [Wm^{-2}]
(c)
(d)
Kaufman et al. (2005)
Christopher et al. (2006)
Yu et al. (2006)
Yu et al. (2006)
Chung et al. (2005)
Bellouin et al. (2005)
Bellouin et al. (2008)
Quaas et al. (2008)
Myhre (2009)
Zhao et al. (2008)
Zhao et al. (2011)
Bellouin et al. (2013)
Su et al. (2013)
Chung et al. (2016)
Mean
Mean ± 1σ
Mean ± 1σ(enhanced)
−1.5 −1.0 −0.5 0.0
−3 −2 −1 0
Aerosol DRF_{PD} [Wm^{-2}]
(e)
(f)
Myhre (2009)
Bellouin et al. (2013)
Kinne et al. (2013)
Ma et al. (2014)
Kinne (2019)
Matus et al. (2019)
Myhre et al. (2013)
Samset et al. (2014)
IPCC AR5
Bellouin et al. (2020)
Mean
Mean ± 1σ
Mean ± 1σ(enhanced)
−0.8 −0.6 −0.4 −0.2 0.0
−1.5 −1.0 −0.5 0.0
Aerosol DRF_{CLI} [Wm^{-2}]
Model
MODIS
CALIPSO
AERONET
PARASOL
OMI
CERES
MISR
Ocean only
Review/collection
This study
This study (enhanced)
Uncertainty (1σ)
Min, max


All sky
Clear sky
(a)
(b)
Remer and Kaufman (2006)
Yu et al. (2006)
Lee et al. (2014)
Zhang et al. (2005)
Zhao et al. (2008)
Zhao et al. (2011)
Henderson et al. (2013)
Matus et al. (2015)
Oikawa et al. (2018)
Matus et al. (2019)
Lacagnina et al. (2017)
Loeb and Su (2010), #1
Loeb and Su (2010), #2
This study
This study (enhanced)
−1.0 −0.5 0.0 0.5 1.0
−2 −1 0 1 2
Aerosol DRE uncertainty [Wm^{-2}]
(c)
(d)
Kaufman et al. (2005)
Christopher et al. (2006)
Yu et al. (2006)
Yu et al. (2006)
Chung et al. (2005)
Bellouin et al. (2005)
Bellouin et al. (2008)
Quaas et al. (2008)
Zhao et al. (2008)
Zhao et al. (2011)
Bellouin et al. (2013)
Chung et al. (2016)
This study
This study (enhanced)
−0.50 −0.25 0.00 0.25 0.50
−1.0 −0.5 0.0 0.5 1.0
Aerosol DRF_{PD} uncertainty [Wm^{-2}]
(e)
(f)
Myhre (2009)
Bellouin et al. (2013)
Kinne et al. (2013)
Kinne (2019)
Matus et al. (2019)
Myhre et al. (2013)
Samset et al. (2014)
IPCC AR5
Bellouin et al. (2020)
This study
This study (enhanced)
−0.4 −0.2 0.0 0.2 0.4
−0.6 −0.3 0.0 0.3 0.6
Aerosol DRF_{CLI} uncertainty [Wm^{-2}]
Model
MODIS
CALIPSO
AERONET
PARASOL
OMI
CERES
MISR
Review/collection
This study
This study (enhanced)
Ocean only

Aan de Brugh, J. M. J., M. Schaap, E. Vignati, F. Dentener, M. Kahnert, M. Sofiev, V. Huijnen, and M. C. Krol, 2011: The European aerosol budget in 2006. *Atmos. Chem. Phys.*, **11 (3)**, 1117–1139, doi:10.5194/acp-11-1117-2011.

Anderson, T. L., 2005: Testing the MODIS satellite retrieval of aerosol fine-mode fraction. *J. Geophys. Res.*, **110 (D18)**, doi:10.1029/2005jd005978.

Bauer, S. E., S. Menon, D. Koch, T. C. Bond, and K. Tsigaridis, 2010: A global modeling study on carbonaceous aerosol microphysical characteristics and radiative effects. *Atmos. Chem. Phys.*, **10 (15)**, 7439–7456, doi:10.5194/acp-10-7439-2010.

Bauer, S. E., D. L. Wright, D. Koch, E. R. Lewis, R. McGraw, L.-S. Chang, S. E. Schwartz, and R. Ruedy, 2008: MATRIX (Multiconfiguration Aerosol TRacker of mIXing state): an aerosol microphysical module for global atmospheric models. *Atmos. Chem. Phys.*, **8 (20)**, 6003–6035, doi:10.5194/acp-8-6003-2008.

Bellouin, N., O. Boucher, J. Haywood, and M. S. Reddy, 2005: Global estimate of aerosol direct radiative forcing from satellite measurements. *Nature*, **438 (7071)**, 1138–1141, doi:10.1038/nature04348.

Bellouin, N., O. Boucher, D. Tanré, and O. Dubovik, 2003: Aerosol absorption over the clear-sky oceans deduced from POLDER-1 and AERONET observations. *Geophys. Res. Lett.*, **30 (14)**, doi:10.1029/2003gl017121.

Bellouin, N., A. Jones, J. Haywood, and S. A. Christopher, 2008: Updated estimate of aerosol direct radiative forcing from satellite observations and comparison against the Hadley Centre climate model. *J. Geophys. Res.*, **113 (D10)**, doi:10.1029/2007jd009385.

Bellouin, N., J. Quaas, J.-J. Morcrette, and O. Boucher, 2013: Estimates of aerosol radiative forcing from the MACC re-analysis. *Atmos. Chem. Phys.*, **13 (4)**, 2045–2062, doi:10.5194/acp-13-2045-2013.

Bellouin, N., J. Rae, A. Jones, C. Johnson, J. Haywood, and O. Boucher, 2011: Aerosol forcing in the Climate Model Intercomparison Project (CMIP5) simulations by HadGEM2-ES and the role of ammonium nitrate. *J. Geophys. Res.*, **116 (D20)**, doi:10.1029/2011jd016074.

Bellouin, N., and Coauthors, 2020: Bounding Global Aerosol Radiative Forcing of Climate Change. *Rev. Geophys.*, **58 (1)**, doi:10.1029/2019rg000660.

Bian, H., M. Chin, J. M. Rodriguez, H. Yu, J. E. Penner, and S. Strahan, 2009: Sensitivity of aerosol optical thickness and aerosol direct radiative effect to relative humidity. *Atmos. Chem. Phys.*, **9 (7)**, 2375–2386, doi:10.5194/acp-9-2375-2009.

Boucher, O., and D. Tanré, 2000: Estimation of the aerosol perturbation to the Earth's Radiative Budget over oceans using POLDER satellite aerosol retrievals. *Geophys. Res. Lett.*, **27 (8)**, 1103–1106, doi:10.1029/1999gl010963.

Boucher, O., and Coauthors, 2013: *Climate Change 2013: The Physical Science Basis. Contribution of Working Group I to the Fifth Assessment Report of the Intergovernmental Panel on Climate Change: Clouds and Aerosols*, chap. 7, 571–658. Cambridge University Press, Cambridge, United Kingdom and New York, NY, USA, doi:10.1017/CBO9781107415324.016.

Burton, S. P., R. A. Ferrare, M. A. Vaughan, A. H. Omar, R. R. Rogers, C. A. Hostetler, and J. W. Hair, 2013: Aerosol classification from airborne HSRL and comparisons with the CALIPSO vertical feature mask. *Atmos. Meas. Tech.*, **6 (5)**, 1397–1412, doi:10.5194/amt-6-1397-2013.

Burton, S. P., M. A. Vaughan, R. A. Ferrare, and C. A. Hostetler, 2014: Separating mixtures of aerosol types in airborne High Spectral Resolution Lidar data. *Atmos. Meas. Tech.*, **7 (2)**, 419–436, doi:10.5194/amt-7-419-2014.

Burton, S. P., and Coauthors, 2016: Information content and sensitivity of the $3\beta + 2\alpha$ lidar measurement system for aerosol microphysical retrievals. *Atmos. Meas. Tech.*, **9 (11)**, 5555–5574, doi:10.5194/amt-9-5555-2016.

Carslaw, K., L. Lee, L. Regayre, and J. Johnson, 2018: Climate Models Are Uncertain, but We Can Do Something About It. *Eos*, **99**, doi:10.1029/2018eo093757.

Cescatti, A., and Coauthors, 2012: Intercomparison of MODIS albedo retrievals and in situ measurements across the global FLUXNET network. *Remote Sens. Environ.*, **121**, 323–334, doi:10.1016/j.rse.2012.02.019.

Chaikovsky, A., and Coauthors, 2016: Lidar-Radiometer Inversion Code (LIRIC) for the retrieval of vertical aerosol properties from combined lidar/radiometer data: development and distribution in EARLINET. *Atmos. Meas. Tech.*, **9 (3)**, 1181–1205, doi:10.5194/amt-9-1181-2016.

Chin, M., R. B. Rood, S.-J. Lin, J.-F. Müller, and A. M. Thompson, 2000: Atmospheric sulfur cycle simulated in the global model GOCART: Model description and global properties. *J. Geophys. Res. Atmospheres*, **105 (D20)**, 24 671–24 687, doi:10.1029/2000jd900384.

Chin, M., and Coauthors, 2002: Tropospheric Aerosol Optical Thickness from the GOCART Model and Comparisons with Satellite and Sun Photometer Measurements. *J. Atmos. Sci.*, **59 (3)**, 461–483, doi:10.1175/1520-0469(2002)059(0461:taotft)2.0.co;2.

Christopher, S. A., J. Zhang, Y. J. Kaufman, and L. A. Remer, 2006: Satellite-based assessment of top of atmosphere anthropogenic aerosol radiative forcing over cloud-free oceans. *Geophys. Res. Lett.*, **33 (15)**, doi:10.1029/2005gl025535.

Chung, C. E., J.-E. Chu, Y. Lee, T. van Noije, H. Jeoung, K.-J. Ha, and M. Marks, 2016: Global fine-mode aerosol radiative effect, as constrained by comprehensive observations. *Atmos. Chem. Phys.*, **16 (13)**, 8071–8080, doi:10.5194/acp-16-8071-2016.

Chung, C. E., V. Ramanathan, D. Kim, and I. A. Podgorny, 2005: Global anthropogenic aerosol direct forcing derived from satellite and ground-based observations. *J. Geophys. Res.*, **110 (D24)**, doi:10.1029/2005jd006356.

Ginoux, P., M. Chin, I. Tegen, J. M. Prospero, B. Holben, O. Dubovik, and S.-J. Lin, 2001: Sources and distributions of dust aerosols simulated with the GOCART model. *J. Geophys. Res. Atmospheres*, **106 (D17)**, 20 255–20 273, doi:10.1029/2000jd000053.

Grosvenor, D. P., and Coauthors, 2018: Remote Sensing of Droplet Number Concentration in Warm Clouds: A Review of the Current State of Knowledge and Perspectives. *Rev. Geophys.*, **56 (2)**, 409–453, doi:10.1029/2017rg000593.

Hair, J. W., and Coauthors, 2008: Airborne High Spectral Resolution Lidar for profiling aerosol optical properties. *Appl. Opt.*, **47 (36)**, 6734–6752, doi:10.1364/AO.47.006734.

Henderson, D. S., T. L'Ecuyer, G. Stephens, P. Partain, and M. Sekiguchi, 2013: A Multisensor Perspective on the Radiative Impacts of Clouds and Aerosols. *J. Appl. Meteor. Climatol.*, **52 (4)**, 853–871, doi:10.1175/jamc-d-12-025.1.

Jin, Y., C. B. Schaaf, C. E. Woodcock, F. Gao, X. Li, and A. H. Strahler, 2003: Consistency of MODIS surface bidirectional reflectance distribution function and albedo retrievals: 2. Validation. *J. Geophys. Res.*, **108 (D5)**, doi:10.1029/2002jd002804.

Jin, Z., T. P. Charlock, W. L. Smith, and K. Rutledge, 2004: A parameterization of ocean surface albedo. *Geophys. Res. Lett.*, **31 (22)**, doi:10.1029/2004gl021180.

Jin, Z., and Coauthors, 2005: Radiative Transfer Modeling for the CLAMS Experiment. *J. Atmos. Sci.*, **62 (4)**, 1053–1071, doi:10.1175/jas3351.1.

Johnson, J. S., and Coauthors, 2018: The importance of comprehensive parameter sampling and multiple observations for robust constraint of aerosol radiative forcing. *Atmos. Chem. Phys.*, **18 (17)**, 13 031–13 053, doi:10.5194/acp-18-13031-2018.

Kahn, R. A., and B. J. Gaitley, 2015: An analysis of global aerosol type as retrieved by MISR. *Journal of Geophysical Research: Atmospheres*, **120 (9)**, 4248–4281, doi:10.1002/2015jd023322.

Kaufman, Y. J., O. Boucher, D. Tanré, M. Chin, L. A. Remer, and T. Takemura, 2005: Aerosol anthropogenic component estimated from satellite data. *Geophys. Res. Lett.*, **32 (17)**, doi:10.1029/2005gl023125.

Kim, M.-H., and Coauthors, 2018: The CALIPSO version 4 automated aerosol classification and lidar ratio selection algorithm. *Atmos. Meas. Tech.*, **11 (11)**, 6107–6135, doi:10.5194/amt-11-6107-2018.

Kinne, S., 2019: Aerosol radiative effects with MACv2. *Atmos. Chem. Phys.*, **19 (16)**, 10 919–10 959, doi:10.5194/acp-19-10919-2019.

Kinne, S., and Coauthors, 2013: MAC-v1: A new global aerosol climatology for climate studies. *J. Adv. Model. Earth Syst.*, **5 (4)**, 704–740, doi:10.1002/jame.20035.

Kirkevåg, A., and Coauthors, 2012: Aerosol-climate interactions in the Norwegian Earth System Model— NorESM. *Geosci. Model Dev.*, **5 (3)**, 2599–2685, doi:10.5194/gmd-6-207-2013.

Knobelspiesse, K., and Coauthors, 2011: Combined retrievals of boreal forest fire aerosol properties with a polarimeter and lidar. *Atmos. Chem. Phys.*, **11 (14)**, 7045–7067, doi:10.5194/acp-11-7045-2011.

Korras-Carraca, M., V. Pappas, N. Hatzianastassiou, I. Vardavas, and C. Matsoukas, 2019: Global vertically resolved aerosol direct radiation effect from three years of CALIOP data using the FORTH radiation transfer model. *Atmos. Res.*, **224**, 138–156, doi:10.1016/j.atmosres.2019.03.024.

Lacagnina, C., O. P. Hasekamp, and O. Torres, 2017: Direct radiative effect of aerosols based on PARASOL and OMI satellite observations. *J. Geophys. Res.*, **122 (4)**, 2366–2388, doi:10.1002/2016jd025706.

Lee, J., J. Kim, and Y. G. Lee, 2014: Simultaneous retrieval of aerosol properties and clear-sky direct radiative effect over the global ocean from MODIS. *Atmos. Environ.*, **92**, 309–317, doi:10.1016/j.atmosenv.2014.04.021.

Lin, G., J. E. Penner, S. Sillman, D. Taraborrelli, and J. Lelieveld, 2012: Global modeling of SOA formation from dicarbonyls, epoxides, organic nitrates and peroxides. *Atmos. Chem. Phys.*, **12 (10)**, 4743–4774, doi:10.5194/acp-12-4743-2012.

Liu, X., and Coauthors, 2012: Toward a minimal representation of aerosols in climate models: description and evaluation in the Community Atmosphere Model CAM5. *Geosci. Model Dev.*, **5 (3)**, 709–739, doi:10.5194/gmd-5-709-2012.

Loeb, N. G., and N. Manalo-Smith, 2005: Top-of-Atmosphere Direct Radiative Effect of Aerosols over Global Oceans from Merged CERES and MODIS Observations. *J. Climate*, **18 (17)**, 3506–3526, doi:10.1175/jcli3504.1.

Loeb, N. G., and W. Su, 2010: Direct Aerosol Radiative Forcing Uncertainty Based on a Radiative Perturbation Analysis. *J. Climate*, **23 (19)**, 5288–5293, doi:10.1175/2010jcli3543.1.

Lopatin, A., O. Dubovik, A. Chaikovsky, P. Goloub, T. Lapyonok, D. Tanré, and P. Litvinov, 2013: Enhancement of aerosol characterization using synergy of lidar and sun-photometer coincident observations: the GARRLiC algorithm. *Atmos. Meas. Tech.*, **6 (8)**, 2065–2088, doi:10.5194/amt-6-2065-2013.

Ma, X., F. Yu, and J. Quaas, 2014: Reassessment of satellite-based estimate of aerosol climate forcing. *J. Geophys. Res.*, **119 (17)**, 10,394–10,409, doi:10.1002/2014jd021670.

Matus, A. V., T. S. L'Ecuyer, and D. S. Henderson, 2019: New Estimates of Aerosol Direct Radiative Effects and Forcing From A-Train Satellite Observations. *Geophys. Res. Lett.*, **46 (14)**, 8338–8346, doi:10.1029/2019gl083656.

Matus, A. V., T. S. L'Ecuyer, J. E. Kay, C. Hannay, and J.-F. Lamarque, 2015: The Role of Clouds in Modulating Global Aerosol Direct Radiative Effects in Spaceborne Active Observations and the Community Earth System Model. *J. Climate*, **28 (8)**, 2986–3003, doi:10.1175/jcli-d-14-00426.1.

McComiskey, A., S. E. Schwartz, B. Schmid, H. Guan, E. R. Lewis, P. Ricchiazzi, and J. A. Ogren, 2008: Direct aerosol forcing: Calculation from observables and sensitivities to inputs. *J. Geophys. Res.*, **113 (D9)**, doi:10.1029/2007jd009170.

Myhre, G., 2009: Consistency Between Satellite-Derived and Modeled Estimates of the Direct Aerosol Effect. *Science*, **325 (5937)**, 187–190, doi:10.1126/science.1174461.

Myhre, G., and Coauthors, 2007: Comparison of the radiative properties and direct radiative effect of aerosols from a global aerosol model and remote sensing data over ocean. *Tellus B*, **59 (1)**, 115–129, doi:10.1111/j.1600-0889.2006.00226.x.

Myhre, G., and Coauthors, 2009: Modelled radiative forcing of the direct aerosol effect with multi-observation evaluation. *Atmos. Chem. Phys.*, **9 (4)**, 1365–1392, doi:10.5194/acp-9-1365-2009.

Myhre, G., and Coauthors, 2013: Radiative forcing of the direct aerosol effect from AeroCom Phase II simulations. *Atmos. Chem. Phys.*, **13 (4)**, 1853–1877, doi:10.5194/acp-13-1853-2013.

Nowottnick, E. P., P. R. Colarco, E. J. Welton, and A. da Silva, 2015: Use of the CALIOP vertical feature mask for evaluating global aerosol models. *Atmos. Meas. Tech.*, **8 (9)**, 3647–3669, doi:10.5194/amt-8-3647-2015.

Oh, H.-R., Y.-S. Choi, C.-H. Ho, and M.-J. Jeong, 2013: Estimation of aerosol direct radiative effects for all-sky conditions from CERES and MODIS observations. *J. Atmos. Sol. Terr. Phys.*, **102**, 311–320, doi:10.1016/j.jastp.2013.06.009.

Oikawa, E., T. Nakajima, T. Inoue, and D. Winker, 2013: A study of the shortwave direct aerosol forcing using ESSP/CALIPSO observation and GCM simulation. *J. Geophys. Res.*, **118 (9)**, 3687–3708, doi:10.1002/jgrd.50227.

Oikawa, E., T. Nakajima, and D. Winker, 2018: An Evaluation of the Shortwave Direct Aerosol Radiative Forcing Using CALIOP and MODIS Observations. *J. Geophys. Res.*, **123 (2)**, 1211–1233, doi:10.1002/2017jd027247.

Omar, A. H., and Coauthors, 2009: The CALIPSO Automated Aerosol Classification and Lidar Ratio Selection Algorithm. *J. Atmos. Oceanic Technol.*, **26 (10)**, 1994–2014, doi:10.1175/2009jtecha1231.1.

Quaas, J., O. Boucher, N. Bellouin, and S. Kinne, 2008: Satellite-based estimate of the direct and indirect aerosol climate forcing. *J. Geophys. Res.*, **113 (D5)**, n/a–n/a, doi:10.1029/2007jd008962.

Remer, L. A., and Y. J. Kaufman, 2006: Aerosol direct radiative effect at the top of the atmosphere over cloud free ocean derived from four years of MODIS data. *Atmos. Chem. Phys.*, **6 (1)**, 237–253, doi:10.5194/acp-6-237-2006.

Roman, M. O., and Coauthors, 2013: Use of In Situ and Airborne Multiangle Data to Assess MODIS- and Landsat-Based Estimates of Directional Reflectance and Albedo. *IEEE Trans. Geosci. Remote Sens.*, **51 (3)**, 1393–1404, doi:10.1109/tgrs.2013.2243457.

Russell, P. B., and Coauthors, 2014: A multiparameter aerosol classification method and its application to retrievals from spaceborne polarimetry. *Journal of Geophysical Research: Atmospheres*, **119 (16)**, 9838–9863, doi:10.1002/2013jd021411.

Samset, B. H., G. Myhre, and M. Schulz, 2014: Upward adjustment needed for aerosol radiative forcing uncertainty. *Nature Climate Change*, **4 (4)**, 230–232, doi:10.1038/nclimate2170.

Samset, B. H., C. W. Stjern, E. Andrews, R. A. Kahn, G. Myhre, M. Schulz, and G. L. Schuster, 2018: Aerosol Absorption: Progress Towards Global and Regional Constraints. *Current Climate Change Reports*, **4 (2)**, 65–83, doi:10.1007/s40641-018-0091-4.

Skeie, R. B., T. K. Berntsen, G. Myhre, K. Tanaka, M. M. Kvalevåg, and C. R. Hoyle, 2011: Anthropogenic radiative forcing time series from pre-industrial times until 2010. *Atmos. Chem. Phys.*, **11 (22)**, 11827–11857, doi:10.5194/acp-11-11827-2011.

Stamnes, S., and Coauthors, 2018: Simultaneous polarimeter retrievals of microphysical aerosol and ocean color parameters from the "MAPP" algorithm with comparison to high-spectral-resolution lidar aerosol and ocean products. *Appl. Opt.*, **57 (10)**, 2394, doi:10.1364/ao.57.002394.

Stier, P., and Coauthors, 2005: The aerosol-climate model ECHAM5-HAM. *Atmos. Chem. Phys.*, **5 (4)**, 1125–1156, doi:10.5194/acp-5-1125-2005.

Stier, P., and Coauthors, 2013: Host model uncertainties in aerosol radiative forcing estimates: results from the AeroCom Prescribed intercomparison study. *Atmos. Chem. Phys.*, **13 (6)**, 3245–3270, doi:10.5194/acp-13-3245-2013.

Stroeve, J., J. E. Box, Z. Wang, C. Schaaf, and A. Barrett, 2013: Re-evaluation of MODIS MCD43 Greenland albedo accuracy and trends. *Remote Sens. Environ.*, **138**, 199–214, doi:10.1016/j.rse.2013.07.023.

Su, W., N. G. Loeb, G. L. Schuster, M. Chin, and F. G. Rose, 2013: Global all-sky shortwave direct radiative forcing of anthropogenic aerosols from combined satellite observations and GOCART simulations. *J. Geophys. Res.*, **118 (2)**, 655–669, doi:10.1029/2012jd018294.

Takemura, T., 2005: Simulation of climate response to aerosol direct and indirect effects with aerosol transport-radiation model. *J. Geophys. Res.*, **110 (D2)**, doi:10.1029/2004jd005029.

Takemura, T., M. Egashira, K. Matsuzawa, H. Ichijo, R. O'ishi, and A. Abe-Ouchi, 2009: A simulation of the global distribution and radiative forcing of soil dust aerosols at the Last Glacial Maximum. *Atmos. Chem. Phys.*, **9 (9)**, 3061–3073, doi:10.5194/acp-9-3061-2009.

Thorsen, T. J., R. A. Ferrare, C. A. Hostetler, M. A. Vaughan, and Q. Fu, 2017: The impact of lidar detection sensitivity on assessing aerosol direct radiative effects. *Geophys. Res. Lett.*, **44 (17)**, 9059–9067, doi:10.1002/2017gl074521.

Thorsen, T. J., R. A. Ferrare, S. Kato, and D. M. Winker, 2020: Aerosol Direct Radiative Effect Sensitivity Analysis. *J. Climate*, **33 (14)**, 6119–6139, doi:10.1175/jcli-d-19-0669.1.

Thorsen, T. J., and Q. Fu, 2015a: Automated Retrieval of Cloud and Aerosol Properties from the ARM Raman Lidar. Part II: Extinction. *J. Atmos. Oceanic Technol.*, **32 (11)**, 1999–2023, doi:10.1175/jtech-d-14-00178.1.

Vignati, E., J. Wilson, and P. Stier, 2004: M7: An efficient size-resolved aerosol microphysics module for large-scale aerosol transport models. *J. Geophys. Res. Atmospheres*, **109 (D22)**, n/a–n/a, doi:10.1029/2003jd004485.

Wang, M., and J. E. Penner, 2009: Aerosol indirect forcing in a global model with particle nucleation. *Atmos. Chem. Phys.*, **9 (1)**, 239–260, doi:10.5194/acp-9-239-2009.

Wang, Z., and Coauthors, 2014: Evaluation of MODIS albedo product (MCD43A) over grassland, agriculture and forest surface types during dormant and snow-covered periods. *Remote Sens. Environ.*, **140**, 60–77, doi:10.1016/j.rse.2013.08.025.

Waquet, F., B. Cairns, K. Knobelspiesse, J. Chowdhary, L. D. Travis, B. Schmid, and M. I. Mishchenko, 2009: Polarimetric remote sensing of aerosols over land. *J. Geophys. Res.*, **114 (D1)**, doi:10.1029/2008jd010619.

Wu, L., O. Hasekamp, B. van Diedenhoven, B. Cairns, J. E. Yorks, and J. Chowdhary, 2016: Passive remote sensing of aerosol layer height using near-UV multiangle polarization measurements. *Geophys. Res. Lett.*, **43 (16)**, 8783–8790, doi:10.1002/2016gl069848.

Xu, L., and J. E. Penner, 2012: Global simulations of nitrate and ammonium aerosols and their radiative effects. *Atmos. Chem. Phys.*, **12 (20)**, 9479–9504, doi:10.5194/acp-12-9479-2012.

Yoshioka, M., and Coauthors, 2019: Ensembles of Global Climate Model Variants Designed for the Quantification and Constraint of Uncertainty in Aerosols and Their Radiative Forcing. *J. Adv. Model. Earth Syst.*, doi:10.1029/2019ms001628.

Yu, H., M. Chin, L. A. Remer, R. G. Kleidman, N. Bellouin, H. Bian, and T. Diehl, 2009: Variability of marine aerosol fine-mode fraction and estimates of anthropogenic aerosol component over cloud-free oceans from the Moderate Resolution Imaging Spectroradiometer (MODIS). *J. Geophys. Res.*, **114 (D10)**, doi:10.1029/2008jd010648.

Yu, H., and Coauthors, 2006: A review of measurement-based assessments of the aerosol direct radiative effect and forcing. *Atmos. Chem. Phys.*, **6 (3)**, 613–666, doi:10.5194/acp-6-613-2006.

Zhang, J., 2005: An analysis of potential cloud artifacts in MODIS over ocean aerosol optical thickness products. *Geophys. Res. Lett.*, **32 (15)**, doi:10.1029/2005gl023254.

Zhang, K., and Coauthors, 2012: The global aerosol-climate model ECHAM-HAM, version 2: sensitivity to improvements in process representations. *Atmos. Chem. Phys.*, **12 (19)**, 8911–8949, doi:10.5194/acp-12-8911-2012.

Zhao, T. X.-P., N. G. Loeb, I. Laszlo, and M. Zhou, 2011: Global component aerosol direct radiative effect at the top of atmosphere. *Int. J. Remote Sens.*, **32 (3)**, 633–655, doi:10.1080/01431161.2010.517790.

Zhao, T. X.-P., H. Yu, I. Laszlo, M. Chin, and W. C. Conant, 2008: Derivation of component aerosol direct radiative forcing at the top of atmosphere for clear-sky oceans. *J. Quant. Spectrosc. Radiat. Transfer*, **109 (7)**, 1162–1186, doi:10.1016/j.jqsrt.2007.10.006.